NASA CONTRACTOR REPORT 177382

Catalytic Distillation Water Recovery Subsystem

P. Budininkas
F. Rasouli

CONTRACT NAS2- 11687
September 1985

NASA

NASA CONTRACTOR REPORT 177382

Catalytic Distillation Water Recovery Subsystem

P. Budininkas
F. Rasouli
GARD Division
Chamberlain Manufacturing Corporation
Niles, Illinois

Prepared for
Ames Research Center
under Contract NAS2-11687

National Aeronautics and
Space Administration

Ames Research Center
Moffett Field, California 94035

NASA CR 117382

CATALYTIC DISTILLATION WATER RECOVERY SUBSYSTEM

Final Report

by

P. Budininkas
F. Rasouli

September, 1985

Prepared Under Contract No. NAS2-11687

by

GARD Division
Chamberlain Manufacturing Corporation
7449 N. Natchez Avenue
Niles, Illinois 60648

for

AMES RESEARCH CENTER

NATIONAL AERONAUTICS AND SPACE ADMINISTRATION

FOREWORD

The development work described herein was conducted by the GARD Division of Chamberlain Manufacturing Corp. during the period of August, 1983 through September, 1985 under NASA Contract NAS2-11687. The Project Engineer was P. Budininkas who was assisted by F. Rasouli. The Contract Technical Monitors were Mark I. Leban and Dr. Theodore Wydeven, NASA Ames Research Center, Moffett Field, California.

TABLE OF CONTENTS

LIST OF FIGURES

LIST OF TABLES

SUMMARY

An integrated engineering breadboard subsystem for the recovery of potable water from untreated urine based on the vapor phase catalytic ammonia removal was designed, fabricated and tested. The subsystem is suitable for a zero-g operation.

The system contains two recycle loops: a liquid loop for vaporizing urine and a vapor/gas loop for catalytic ammonia removal. A design analysis, based on thermodynamic, heat transfer and mass flow calculations, correlating the operating parameters with component sizing, configuration and integration into a subsystem was performed to determine conditions minimizing volume, weight and power requirements.

A subsystem based on optimum parameters identified in the design analysis was fabricated using commercially available components. Although volume and weight of the subsystem were minimized, use of commercial components precluded the optimization.

The subsystem was tested to demonstrate the integrated operation and the quality of the recovered water. The testing program consisted of parametric tests, one month of daily tests, and a continuous test of 168 hours of duration.

The integrated engineering breadboard subsystem produces water of very good quality. The recovered water is clear, odorless, low in ammonia and organic carbon, and requires only an adjustment in its pH to meet potable water standards. If further developed, the vapor phase catalytic ammonia removal process would also be competitive with other water recovery systems in weight, volume and power requirements.

INTRODUCTION

Since recovery of potable water from urine and wash water offers great potential for weight and volume savings in manned spaceflights of long duration, considerable effort has been put into the development of water recovery systems. Two distillation processes, Vapor Compression Distillation (VCD) and Thermoelectric Integrated Membrane Evaporation System (TIMES), have evolved into development hardware. Both of these methods are based on the physical processes of evaporation and condensation; therefore, impurities (such as ammonia and volatile organics) vaporizing with water will also be co-condensed with the recovered water. For this reason, these processes require the use of expendable pre- and post-treatment chemicals for the removal of ammonia and organics in the product water.

The catalytic distillation concept is based on the catalytic chemical process where the volatile impurities vaporizing with water are oxidized to innocuous gaseous products. This concept employs two catalyst beds which sequentially first oxidize vapor phase ammonia to a mixture of nitrous oxide (N_2O) and nitrogen (N_2) and organic vapor to carbon dioxide, then decompose the N_2O to nitrogen (N_2) and oxygen (O_2). The advantage of this concept is that no expendable pre- and post-treatment chemicals are required. In addition, because the vaporizing urine is maintained above the pasteurization temperature and its vapor is passed through a catalytic reactor maintained at 250°C, bacterial viability is destroyed or, at least, greatly inhibited.

Previous laboratory bench scale investigations (NAS2-9219, NAS2-9715, NAS2-10237) have demonstrated this catalytic process on ammonia-vapor streams and on urine-vapor streams.

The objective of this program was to design, develop, fabricate, and test an integrated engineering breadboard subsystem for the recovery of potable water from untreated urine. The subsystem utilizes commercially available components and, thus, is not optimized for weight, volume and power requirements; however, its design incorporates a zero-g operating capability. The primary functions of the engineering breadboard subsystem are to demonstrate the integrated operation and the quality of the recovered water; also, gain experimental experience which could be utilized for the design of an optimized subsystem.

To achieve the above objectives, the program consisted of the following main tasks:

1. Subsystem Design.- An analysis of the basic system consisting of a urine recycle loop and a vapor/gas recycle loop was performed using

thermodynamic and heat transfer considerations. Three methods of vapor addition to the vapor/gas recycle loop were considered, then the effects of independent variables on the overall energy requirements for each method were calculated, and a configuration resulting in the lowest energy requirements was selected.

2. Subsystem Fabrication.- Based on the design calculations, individual components were fabricated from commercially available materials and parts, then integrated into a compact and overall subsystem. To conform to customary commercial dimensions, slight changes were made in the theoretically calculated dimensions.

3. Subsystem Testing.- The integrated subsystem was tested using untreated urine. The following test series were performed:

a. Parametric testing
b. Endurance testing consisting of one month of daily tests
c. Continuous test of 168 hours duration.

TABLE OF NOMENCLATURE

Abbreviation	Term
A	Membrane area
D	Inside diameter of the tube
D_e	Equivalent diameter
D_H	Average diameter of the helix
d_i	Inside diameter of the fibers or tubes
d_o	Outside diameter of the fibers or tubes
f	Fanning friction factor
g_c	Gravitational conversion factor
h_i	Heat transfer coefficient for inside fluid
h_{ic}	Corrected heat transfer coefficient
h_o	Heat transfer coefficient for outside fluid
J	Vapor flux through the membrane
j_H	Colburn factor
K	Permeability
k	Fluid thermal conductivity
K_G	Mass transfer coefficient
L	Length of the path
M_v	Vapor molecular weight
N	Number of fibers
N_{Pr}	Prandtl number
N_{Re}	Reynolds number
P_1, P_2	Partial pressure of vapor inside and outside
P_c	Partial pressure of vapor at the condensate film
P_v	Partial pressure of vapor in the gas body
T_c	Temperature of the condensate film
T_g	Temperature of the gas
T_w	Temperature of the coolant
U	Overall heat transfer coefficient
W	Mass flow rate
ε	Pipe roughness
ΔP	Pressure drop
λ	Latent heat
ρ	Fluid density

SUBSYSTEM DESIGN

Energy Management

One of the main objectives of the design phase was to develop an overall process scheme that will minimize the energy requirements. For the catalytic water recovery system, the latent heat of evaporation comprises the largest portion of the total process energy. Proper and effective use of the latent and sensible heats in the process will decrease the overall energy requirement of the system. According to the Second Law of Thermodynamics, the spontaneous transfer of energy takes place only in one direction: from high to low temperatures. Any energy available at a low temperature may be non-usable; in addition, rejecting it to the cabin atmosphere constitutes a penalty. Therefore, a careful thermodynamic analysis of the overall process must be performed to evaluate various possible heat management methods.

A computer program representing the process was developed for calculating the overall energy requirements and changes resulting from various energy management techniques. This program performs a thermodynamic analysis of the overall process by considering mass flow rates, energy transfer rates, temperatures required for the operation of certain components (catalytic reactors, evaporator, condenser) and resultant temperatures at various locations, taking into account fixed parameters listed in Table 1. All other parameters are dependent and can be varied to minimize the energy, weight and volume of the system; these parameters are listed in Table 2. Operationally, the dependent variables are subject to the following constraints:

1. The upper limit of the evaporation temperature is about 353°K (176°F); heating urine to higher temperatures causes a release of gases that tend to form bubbles in the urine recycle loop. The lower limit of the evaporation temperature is decided by the ability of the compressor to create the required pressure in the evaporator.

2. Urine recycle loop acts as a coolant for the condenser; therefore, the condensation temperature is partially related to the evaporation temperature. The approach temperature between the liquid cycle entering the condenser and the gas leaving the condenser sets the condensation temperature.

3. The presence of at least 21% non-condensible gases in the recycle stream restricts the lower boundary of the evaporator pressure.

TABLE 1

FIXED PARAMETERS

Water Recovery Rate, kg/hr	0.546
Temperature of the NH_3 Oxidation Catalyst, °K (°F)	523 (482)
Temperature of the N_2O Decomposition Catalyst, °K (°F)	723 (842)
Inlet Temperature of Urine, °K (°F)	308 (95)
Inlet Temperature of Oxygen, °K (°F)	298 (77)
Exit Temperature of Recovered Water, °K (°F)	308 (95)
Exit Temperature of Vent Gas, °K (°F)	308 (95)
Solids in Urine, %	15
Oxygen in Recycle Stream, %	9

TABLE 2

RANGES OF DEPENDENT VARIABLES

Evaporation Temperature, °K (°F)	338 - 363 (149-194)
Condensation Temperature, °K (°F)	343 - 373 (158-212)
Compression Ratio	2 - 3.5
Evaporator Pressure, MPa	0.029 - 0.1013

4. The combined effect of the evaporator pressure and the compression ratio should be such as to provide a positive head for the vent gas in the recycle stream (i.e., slightly above one atmosphere).

In our calculations, an 85% efficiency of heat recovery, polytropic compression of vapor, and motor/compressor of 85% efficiency were assumed. The physical properties of the fluids are listed in Table 3.

The performance and the energy requirement of the system depend, to a large extent, on the operating conditions and location of the blower/compressor. The compressor has three functions: to increase the partial pressure of vapor entering the condenser, to preheat the vapor/gas stream entering the NH_3 decomposition reactor, and to recirculate the gas stream. To determine the overall configuration giving the optimum energy management, three mixing arrangements around the compressor were considered and the computer program was properly modified for calculating the energy requirement for each case.

Case 1. Blowing Recycle Gas Through the Evaporator.- The basic schematic of a catalytic distillation water recovery system utilizing the evaporator for mixing the urine vapor with recycle gas is depicted in Figure 1. In this configuration, the recycle vapor/gas stream flows through the evaporator and mixes with the permeated vapor. The resultant mixture is compressed in a compressor and passes a recuperator for exchanging heat with the hot stream leaving the NH_3 oxidation reactor. If required, the mixture is further heated to 523°K (482°F) by a heater before entering the NH_3 oxidation reactor.

The effects of different parameters on the energy requirements of the system were investigated by fixing the condensation and evaporation temperatures to selected values, and varying the evaporator pressure and/or the compression ratio. The total evaporator pressure determines the partial pressure of the water vapor in the evaporator, and the compression ratio sets the vapor partial pressure of the mixture entering the condenser. Table 4 presents the values and combinations of variables that were studied.

The effect of the compression ratio on the energy requirement of the system were studied at evaporation temperatures of 338, 343, 353 and 363°K (149, 158, 176 and 194°F) and various evaporator pressures. Examples of typical results are presented in Figure 2 and indicate that at a given pressure the specific energy of the system passes through a minimum with an increase in the compression ratio. Figure 2 also shows that these minimums shift toward the higher compression ratios with an increase in the evaporator pressures. In other words, the benefits of a higher compression ratio offset the increase in the compressor power requirement up to a certain compression ratio; further increase in the compression

TABLE 3

PHYSICAL PROPERTIES OF FLUIDS

Vapor Viscosity, 343°K (158°F)	109.3×10^{-7} Pa.s
Vapor Thermal Conductivity, 343°K (158°F)	2.13×10^{-5} kJ/s.m°K
Vapor Heat Capacity	2.04 kJ/kg.°K
Gas Viscosity, 343°K (158°F)	127.8×10^{-7} Pa.s
Gas Thermal Conductivity, 343°K (158°F)	2.86×10^{-5} kJ/s.m.°K
Gas Heat Capacity	1.04 kJ/kg.°K
Urine Density	1070 kg/m^3
Urine Viscosity, 353°K (176°F)	0.35×10^{-3} Pa.s
Urine Thermal Conductivity	0.708 kJ/s.m°K
Urine Heat Capacity	4.2 kJ/kg.°K

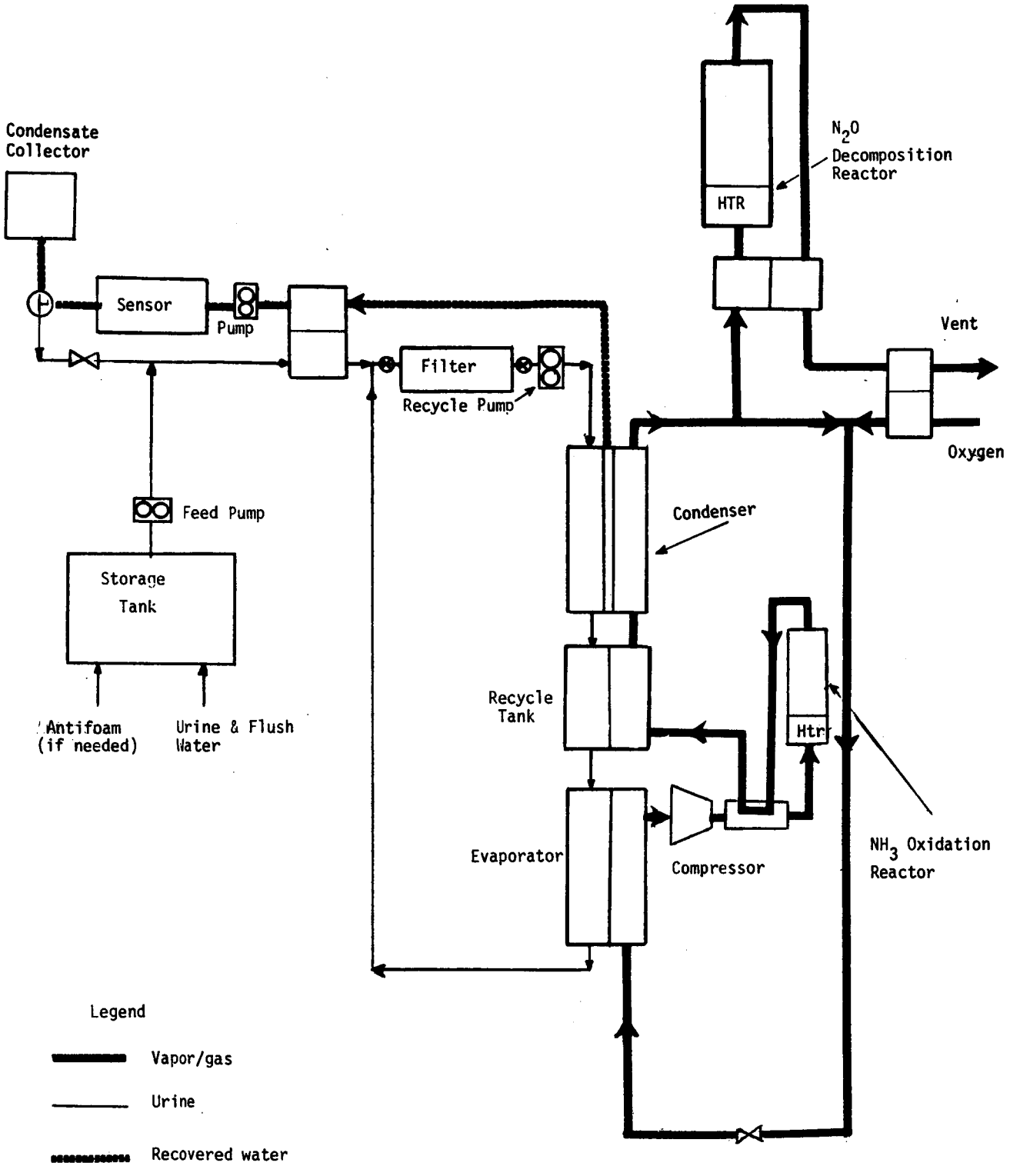

Figure 1 SCHEMATIC OF A SYSTEM FOR PASSING RECYCLE GAS THROUGH EVAPORATOR

TABLE 4

SYSTEMS VARIABLES FOR CASE 1

Evaporation Temperature, °K (°F)	Condensation Temperature, °K (°F)	Compression Ratio	Evaporator Pressure, MPa
338 (149)	348 (167)	2.8	0.029, 0.0317, 0.035, 0.0417, 0.05
		2.59	0.029, 0.0317, 0.035, 0.04, 0.05
		2.39	0.029, 0.0317, 0.035, 0.04, 0.05
		2.23	0.029, 0.0317, 0.04, 0.05
		2.13	0.0317, 0.04, 0.05, 0.07
	343 (158)	2.2	0.029, 0.317, 0.0357, 0.0385, 0.0417
		2.13	0.029, 0.317, 0.0357, 0.0385, 0.0417
343 (158)	353 (176)	2.26	0.04, 0.417, 0.05, 0.07, 0.1013
		2.13	0.04, 0.042, 0.05, 0.07, 0.1013
	348 (167)	2.56	0.04, 0.045, 0.05
		2.5	0.04, 0.045, 0.05
		2.4	0.04, 0.045, 0.05
		2.2	0.04, 0.045, 0.05
		2.13	0.04, 0.045, 0.05
353 (176)	363 (194)	2.4	0.06, 0.07, 0.09, 0.1013
		2.2	0.06, 0.07, 0.09, 0.1013
		2.13	0.06, 0.07, 0.09, 0.1013
		2	0.06, 0.07, 0.09, 0.1013
	362 (192)	2.13	0.06, 0.07, 0.09, 0.1013
	360 (189)	2.13	0.06, 0.07, 0.09, 0.1013
	358 (185)	2.13	0.06, 0.07, 0.09, 0.1013
363 (194)	373 (212)	2.13	0.09, 0.1013

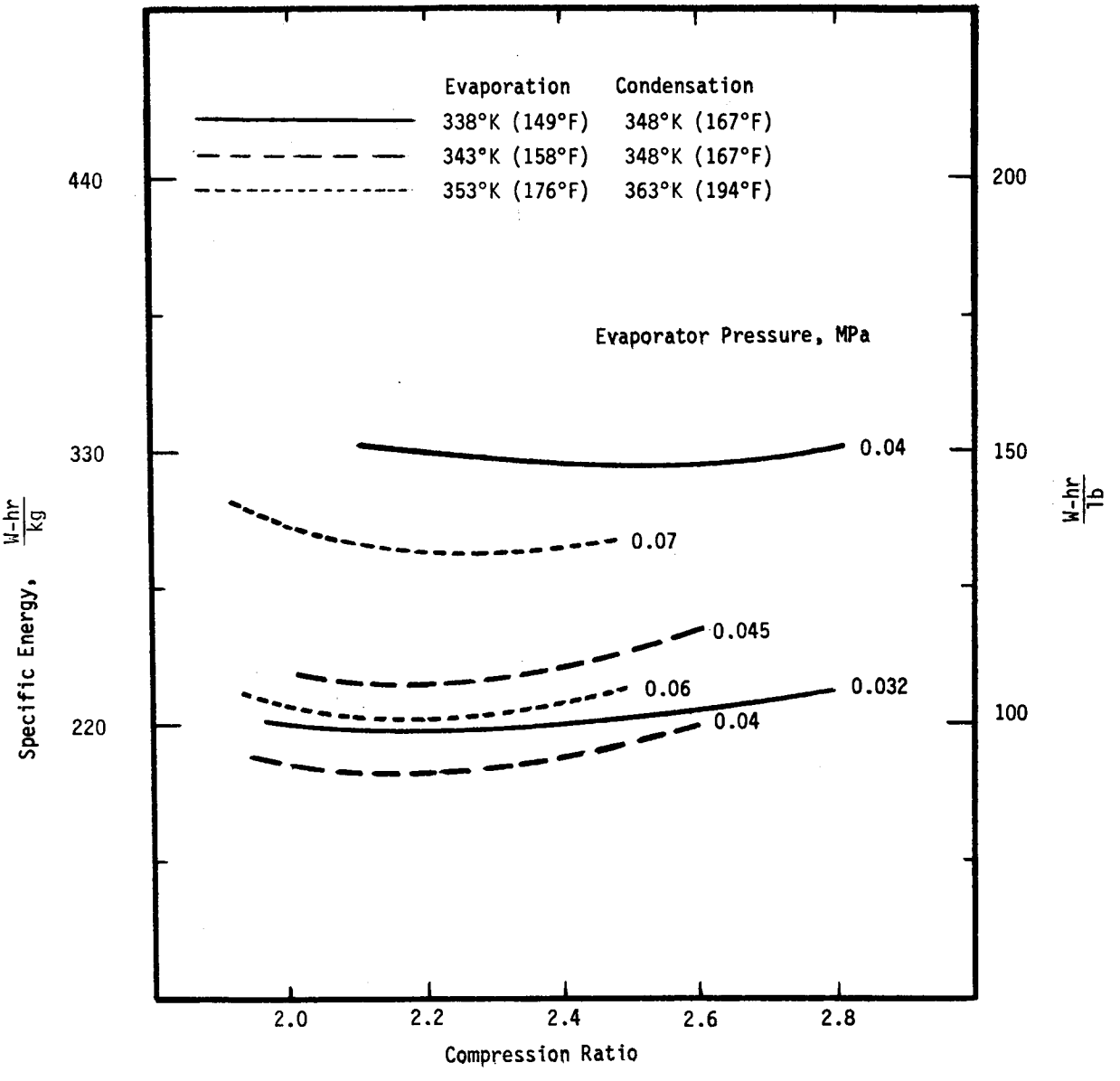

Figure 2 EFFECT OF COMPRESSION RATIO FOR CASE 1

ratio only results in a higher specific energy for the system.

The effects of the evaporator total pressure on the energy requirements of the system were calculated for several evaporation temperatures. The calculations were carried out by assuming a condensation temperatures 10°K above the evaporation temperature in each case, and a compression ratio of 2.13. The results are presented in Figure 3. As can be seen, at a given evaporation temperature, the required specific energy decreases with the decrease in the evaporator total pressure. Furthermore, at a given total pressure, the energy requirement of the system decreases with an increase in the evaporation temperature.

The effects of the condensation temperature on the energy requirements of the system were studied by making several computer runs at evaporation temperatures of 353°K (176°F) and 343°K (158°F) and various condensation temperatures. The energy requirements at various condensation temperatures and evaporator pressures are presented in Figure 4, indicating an increase in the energy requirements of the system with an increase in the condensation temperature, as expected.

Based on the effects of the individual parameters, the following conclusions can be made:

1. Condenser Temperature.- At a given evaporation temperature, the energy requirements of the system decrease with a decrease in the condensation temperature.

2. Evaporator Temperature.- At a given total evaporation pressure, the energy requirements of the system decrease with an increase in the evaporation temperature.

3. Evaporator Pressure.- The energy requirements of the system decrease with a decrease in the evaporator total pressure for each given evaporation temperature.

4. Compression Ratio.- At a given evaporator pressure, the energy requirement of the system passes through a minimum with an increase in the compression ratio.

Case 2. Mixing of Compressed Vapor with the Recycle Stream After the Compressor.- In this configuration, vapor permeated through the hollow fiber membranes is compressed by a compressor to a pressure slightly above the gas recycle stream pressure and mixed with the recycle stream which is circulated by a small blower. The resultant mixture then follows a path similar to the previous case; however, the gas stream remains at a higher pressure. The schematic diagram of this arrangement is shown in Figure 5.

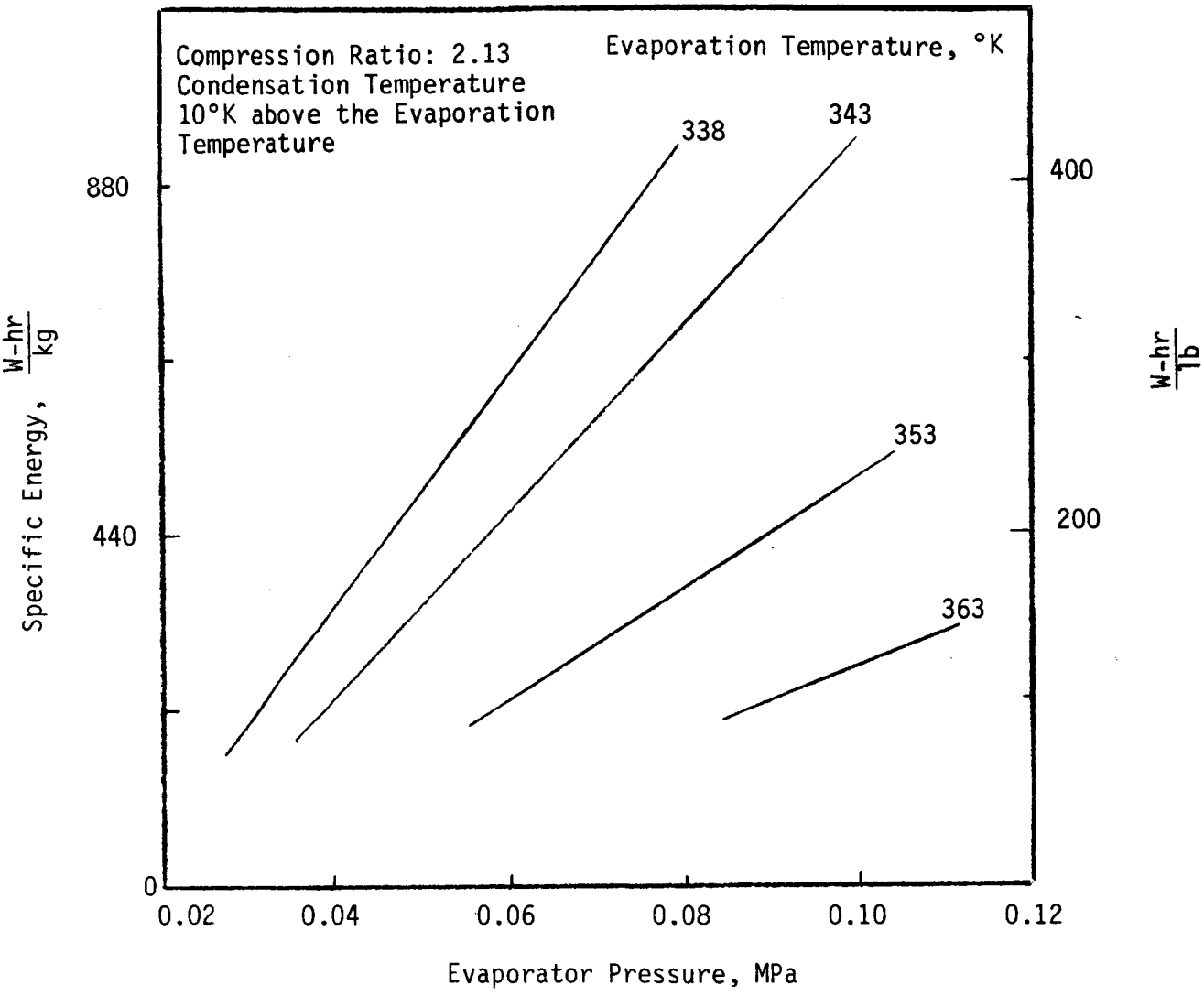

Figure 3 EFFECT OF EVAPORATOR PRESSURE

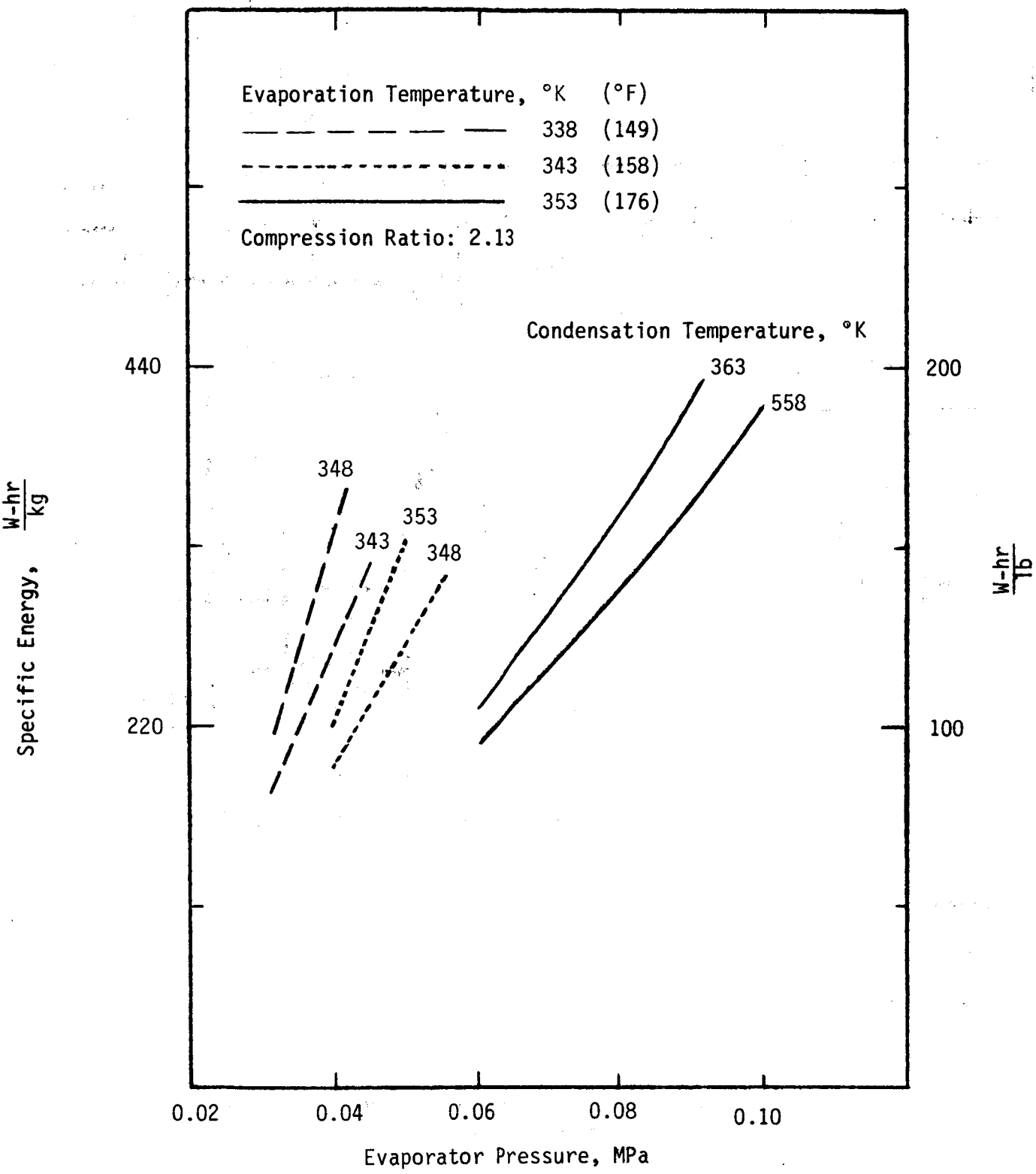

Figure 4 EFFECT OF CONDENSATION TEMPERATURE

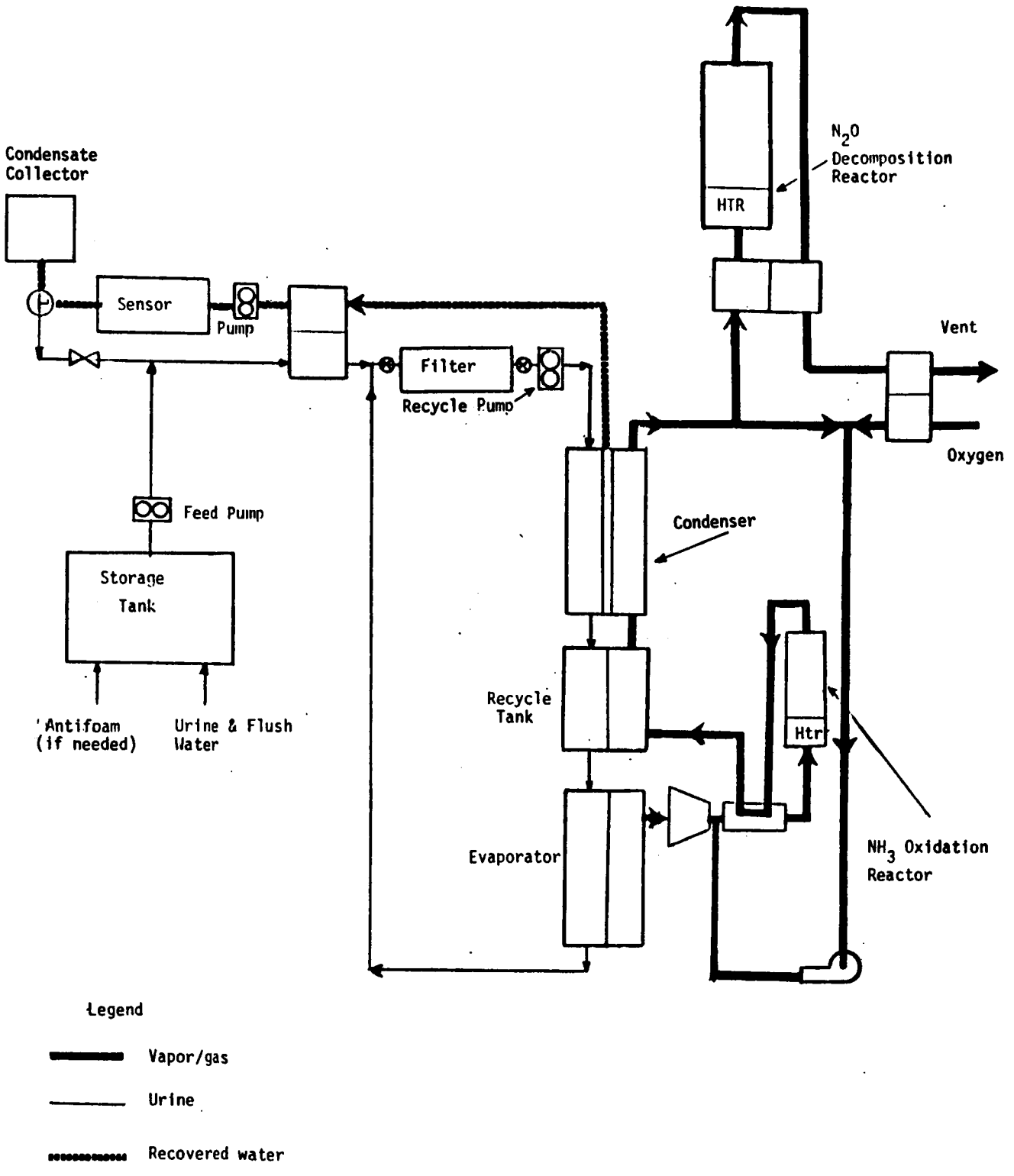

Figure 5 SCHEMATIC OF A SYSTEM MIXING COMPRESSED VAPOR WITH THE RECYCLE STREAM

To determine the effects of the operating parameters on the energy requirements of this arrangement, several computer runs were made at evaporation temperatures of 338, 343, and 353°K. To fully express the system, the evaporation and condensation temperatures, the percentage of non-condensables and the pressure in the recycle stream must be specified. The recycle stream pressure, in turn, determines the compression ratio and the partial pressure of the mixture entering the condenser. The values of parameters that were studied are listed in Table 5.

The effects of the compression ratio on the energy requirements of the system are illustrated in Figure 6. As can be seen, at a given vapor percentage, the energy requirement decreases with an increase in the compression ratio. This behavior can be attributed to the higher vapor partial pressures obtained at higher compression ratios. The results also show that despite the elimination of the unnecessary recompression of the recycle stream, the overall energy requirements of the system are not lower than in the previous case. This is because additional energy is required for heating the recycle stream to the temperature of the NH_3 oxidation reactor and for recirculation of gas through the system by a blower.

The effects of the condensation temperature on the energy requirements of the system were calculated at evaporation temperatures of 338 and 343°K (149 and 158°F). Similarly to Case 1, the specific energy decreases with a decrease in the condensation temperature.

Case 3. Mixing Vapor and Recycle Gas Before the Compressor.- In this configuration, the recycle stream is mixed with low pressure vapor produced by the evaporator in a mixing chamber before being compressed by the compressor. Figure 7 shows this schematic of this arrangement.

The concept and energy calculation procedure for Cases 1 and 3 are similar, except for some minor differences; therefore, it can be anticipated to obtain identical results for both cases under similar operating conditions. The energy calculations for the two cases operated under several identical conditions verify this similarity.

Summary.- The conditions corresponding to the minimum energy requirements of the system can be determined by combining the effects of all parameters. The energy requirements can be lowered by decreasing the condensation temperature; however, the interdependence of the temperatures of condensation and evaporation limits the extent of the decrease in condensation temperature. The lower practical condensation temperature is 343°K (158°F), and it corresponds to an evaporation temperature of 338°K (149°F). Therefore, the optimum compression ratio and evaporator pressures must be considered for these evaporation and condensation temperatures.

TABLE 5

SYSTEMS VARIABLES FOR CASE 2

Evaporation Temperature, °K (°F)	Condensation Temperature, °K (°F)	Recycle Pressure, MPa	% Vapor at the Reactor Entrance
338 (149)	348 (167)	0.6 0.075 0.087	0.8, 0.78, 0.69, 0.6 0.8, 0.7, 0.65 0.8, 0.68, 0.66
	343 (158)	0.087	0.78, 0.74, 0.69, 0.66
343 (158)	353 (176)	0.109 0.093 0.078 0.084	0.78, 0.69, 0.64 0.8, 0.66, 0.64 0.8, 0.77, 0.68, 0.65 0.8, 0.77, 0.7, 0.66
	348 (167)	0.109	0.8, 0.74, 0.69, 0.64
353 (176)	363 (194)	0.166 0.142 0.118	0.8, 0.78, 0.7, 0.65 0.8, 0.76, 0.59, 0.55 0.79, 0.76, 0.7, 0.6

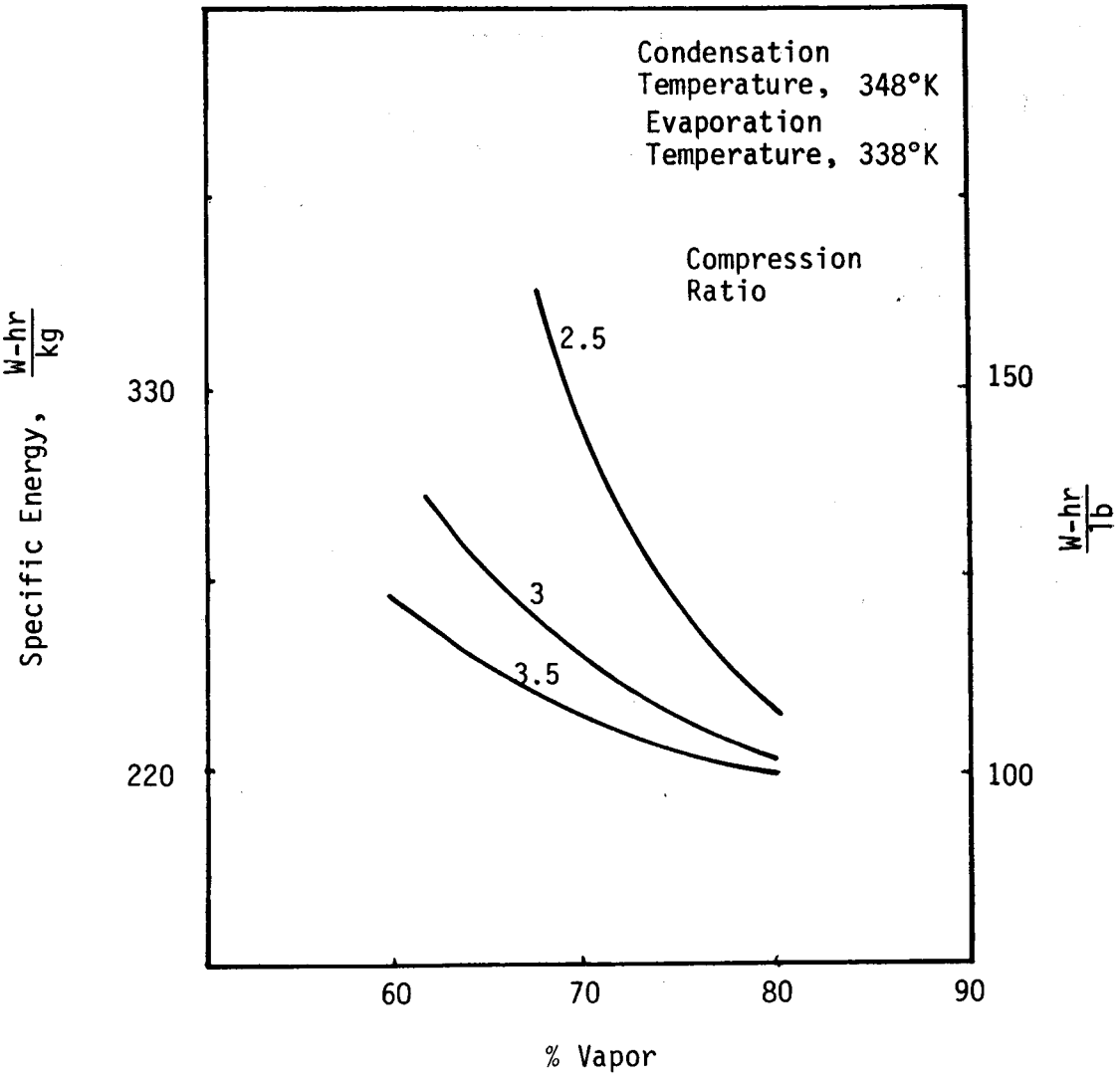

Figure 6 EFFECT OF COMPRESSION RATIO FOR CASE 2

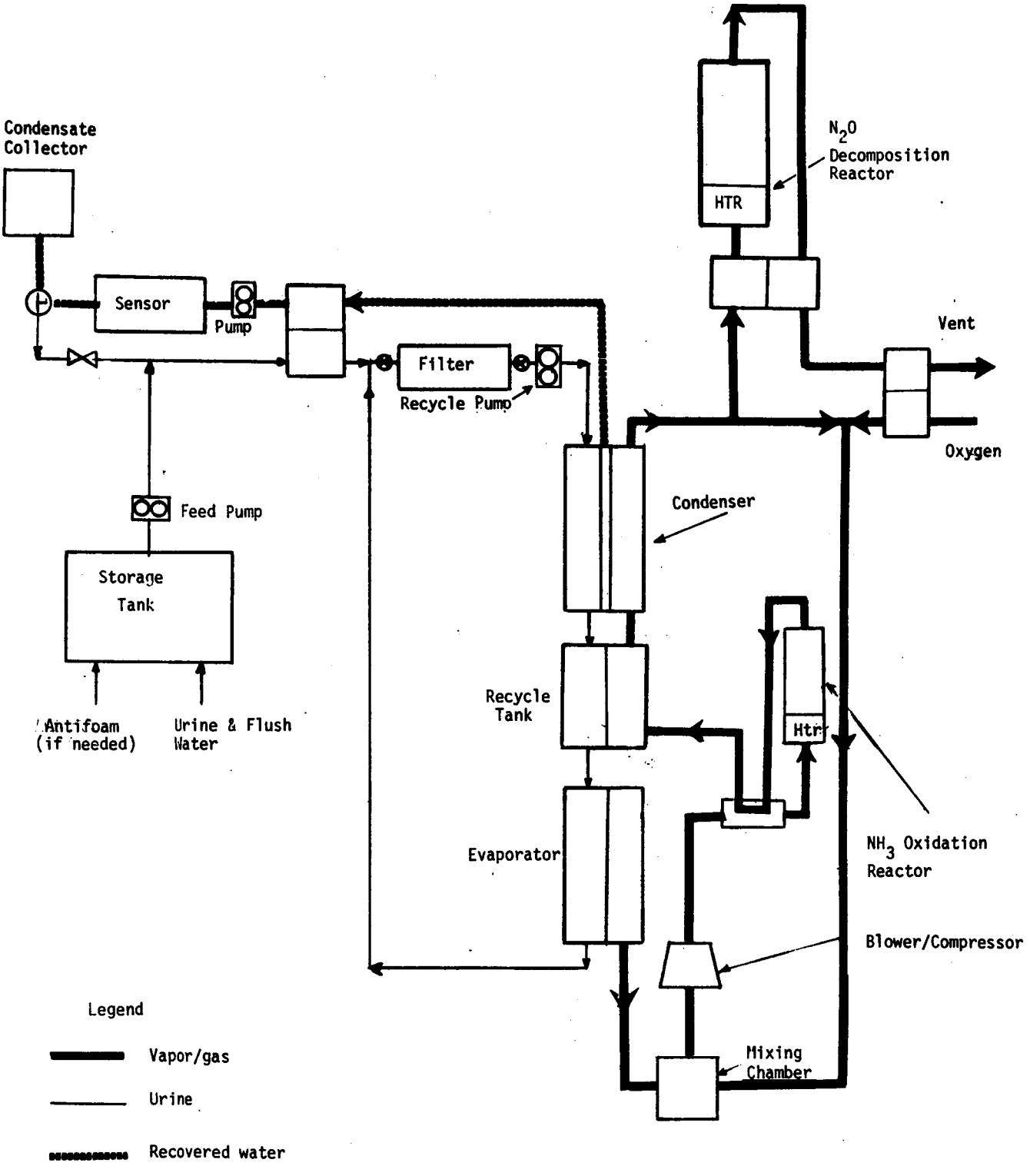

Figure 7 SCHEMATIC OF A SYSTEM FOR MIXING VAPOR WITH RECYCLE GAS BEFORE THE COMPRESSOR

The energy requirements for the three system configurations operating at optimum conditions are shown in Table 6. Among the three mixing arrangements, Case 1 is the most attractive because of its low energy requirements and mechanical and operational feasibility. Case 2 has the following disadvantages: a) need for a blower to recirculate the gas stream, b) need for a heater for superheating the vapor before compression. Case 3 is essentially the same as Case 1 for energy considerations; however, it has an operational problem associated with mixing of high and low pressure vapor/gas streams.

The conditions corresponding to the minimum energy requirements are not necessarily the best practical conditions. The problems with operating the system under the conditions resulting in minimum energy requirements are:

a) Operation of the gas recycle stream below atmospheric pressure

b) Difficulties in obtaining a compressor capable of creating the adequate suction for the required flow rate.

Operational difficulties can be eliminated by operating the system at the following conditions:

Evaporation temperature, 343°K (158°F)
Condensation temperature, 348°K (167°F)
Compression ratio, 2.56
Evaporator pressure, 0.04 MPa

The most practically feasible design conditions for the temperatures and pressure are shown in Figure 8. To be on the safe side, conditions that are somewhat harsher than optimum were used in these design calculations.

Design of System Components

The individual components of the system are designed to implement the configuration and operating parameters identified in the previous section. The size and configuration of each componnet are designed for a three-man water recovery rate, highest possible heat recuperation under the process conditions, and minimal electrical energy requirements.

Catalytic Reactors.- The ammonia oxidation and the nitrous oxide decomposition reactors operate at high temperatures, 523°K (482°F) and 723°K (842°F) respectively. A proper reactor design should include a heat exchanger to utilize the energy of the hot mixtures leaving the reactor to preheat the incoming feeds. In addition, the reactor assembly should have the following construction and operational features:

TABLE 6

ESTIMATE OF ENERGY REQUIREMENTS FOR THE OPTIMUM AND BEST OPERATIONAL CONDITIONS

Energy	Requirements					
	Cases 1* & 3		Case 2**		Best Operational Case 1***	
	W-h/kg	W-h/lb	W-h/kg	W-h/lb	W-h/kg	W-h/lb
a) Energy Needs W/O Recuperation						
Heating of urine	680.1	308.5	690.7	313.3	696.2	315.8
Heating gas/vapor after Compression to NH_3 reactor temperature	68.6	31.1	32.4	14.7	26.5	12.0
Preheating oxygen	0.7	0.3	0.5	0.2	0.7	0.3
Heating gas to N_2O decomposition temperature	5.5	2.5	4.8	2.2	4.6	2.1
Compressor	119.9	54.4	131.6	59.7	150.1	68.1
Liquid pumps	55.1	25.0	55.1	25.0	55.1	25.0
Gas Blower	–	–	3.7	1.7	–	–
Total	929.9	421.8	918.8	416.8	933.2	423.3
b) Energy Saving by Recuperation						
Feed/product heat exchanger	34.6	15.7	34.6	15.7	39.4	17.9
Condenser	561.3	254.6	565.0	256.3	562.0	254.9
Recycle tank heat exchanger	83.8	38.0	90.4	41.0	95.0	254.9
Oxygen/vent gas heat exchanger	0.7	0.3	0.5	0.2	0.7	0.3
N_2O reactor heat exchanger	4.4	2.0	3.3	1.5	4.0	1.8
NH_3 reactor heat exchanger	49.6	22.5	19.6	8.9	15.0	6.8
Total	734.4	333.1	713.4	323.6	716.1	324.8
c) Energy Required with Recuperation	195.5	88.7	205.4	93.2	217.1	98.5

*Evaporation Temperature = 338°K, Condensation Temperature = 343°K, Evaporator Pressure = 0.032 MPa, Non Condensables = 21%, Compression Ratio = 2.13

**Evaporation Temperature = 338°K, Condensation Temperature = 343°K, Evaporator Pressure = 0.087 MPa, Non Condensables = 21%, Compression Ratio = 3.5

***Evaporation Temperature = 343°K, Condensation Temperature = 348°K, Evaporator Pressure = 0.04 MPa, Non Condensables = 22%, Compression Ratio = 2.56

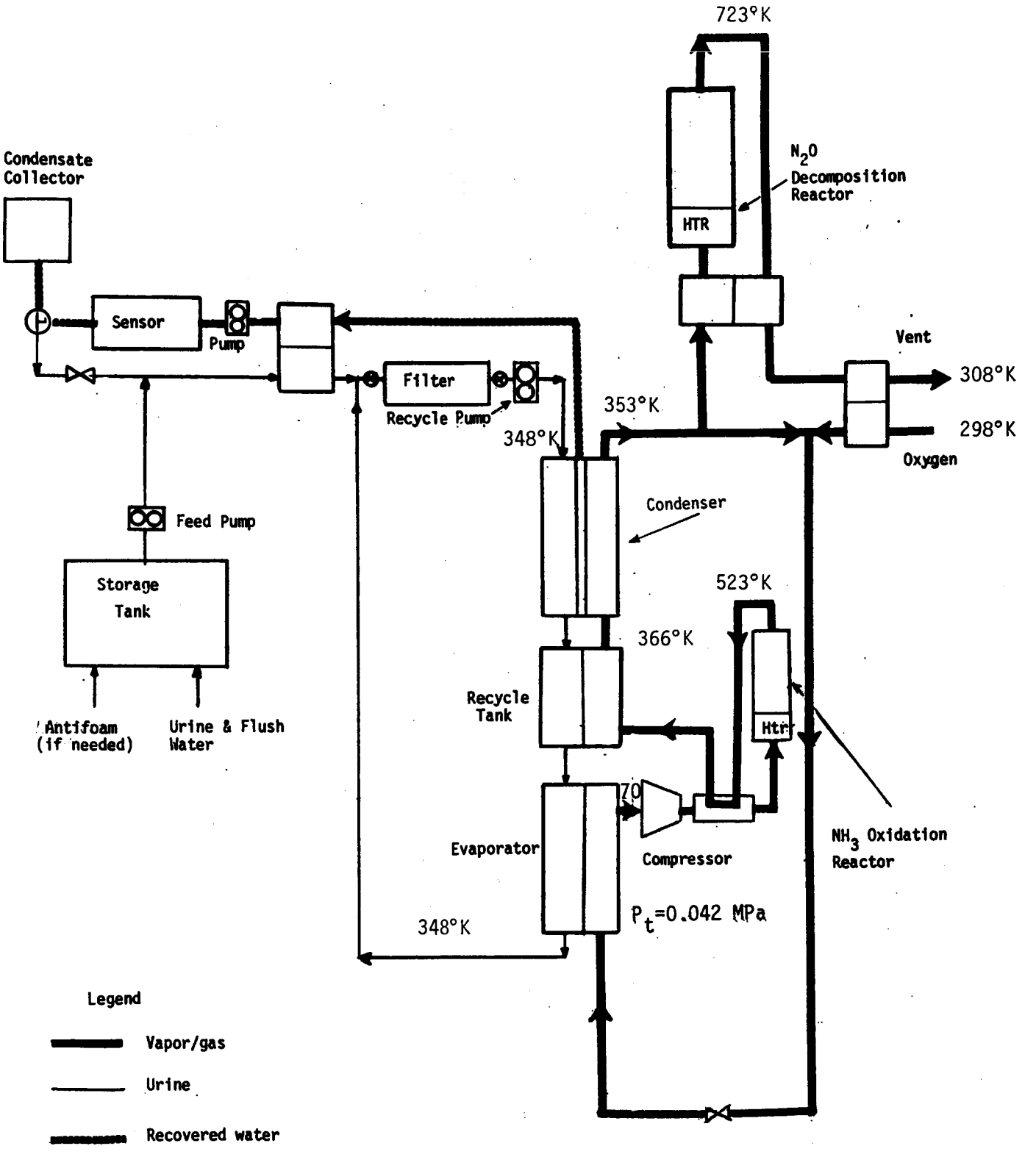

Figure 8 SYSTEM DESIGN CONDITIONS

a) A proper heating element for preheating the reactor during the start-up and for maintaining the required operational temperatures under the respective flow conditions,

b) Catalyst supports below and above the catalyst bed to promote mixing and heating of feed mixture,

c) Thermocouples near the inlet, midpoint, and the outlet of the catalyst bed for measuring and controlling the temperature.

Under the anticipated operating conditions, a combined reactor and helical coil heat exchanger is a suitable choice that can provide the necessary surface area for heat transfer in a limited space. This type of heat exchanger consists of a coil fabricated from a stainless steel tube which is fitted in the annular portion of two concentric cylinders. The inside cylinder contains the catalyst and serves as the reactor. The gas stream leaving the reactor flows through the annulus to preheat the feed flowing inside the coil. A schematic cutaway view of the reactor/heat exchanger is shown in Figure 9. Heating the gas stream in the NH_3 oxidation reactor does not seem to be a problem, but a special arrangement should be made for heating the N_2O decomposition reactor, because of a low gas flow rate. Both reactors are properly insulated to reduce the heat losses.

The design requirements and conditions for three-man sized reactors are summarized in Table 7. These parameters are based on the processing rate required for a three-man crew and experience with previously tested catalytic reactors for oxidation of ammonia and for decomposition of nitrous oxide. Each reactor is sized to contain a slightly larger catalyst bed than required. The ammonia oxidation reactor contains 220 cm^3 and the nitrous oxide decomposition reactor 55 cm^3 of appropriate catalyst material.

The inner tube diameter is determined from the volume of the catalyst bed and the optimum length to diameter ratio. The diameter of the heat exchanger coil is obtained by the velocity of the fluid inside the coil needed to meet heat transfer and pressure drop requirements. The minimum clearances between the annulus walls and the coil, and between two consecutive turns of the coil should be equal. In our calculations of the inside diameter, both clearances are taken as one-half of the outside diameter of the coil. Standard size tubing close to the calculated dimensions is selected and the clearances are properly adjusted with the new dimensions.

The heat-transfer coefficient in the annulus, h_o, is calculated using the following equation:

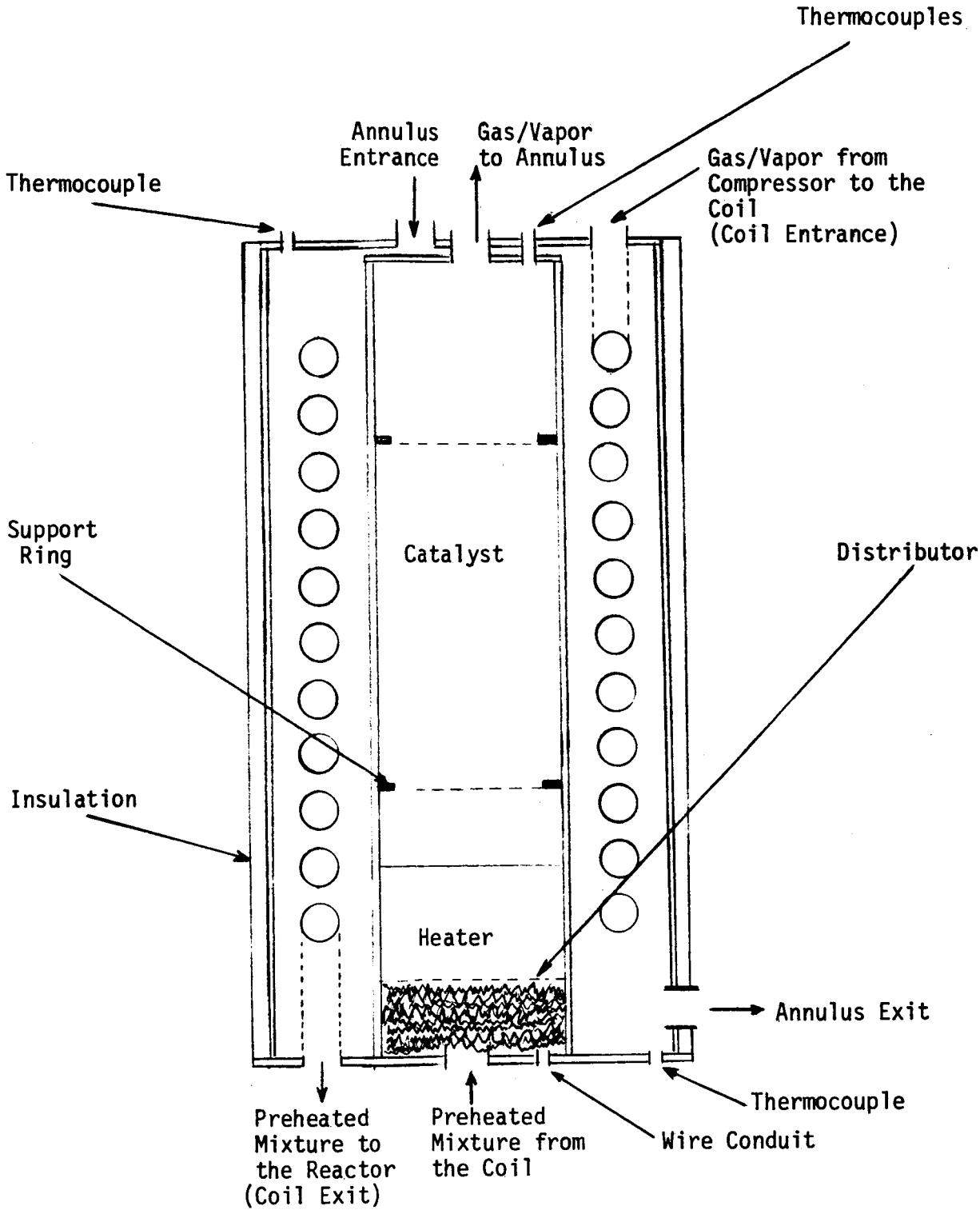

Figure 9 REACTOR/HEAT EXCHANGER ASSEMBLY

TABLE 7

CATALYTIC REACTOR DESIGN PARAMETERS

a) NH_3 Oxidation Reactor Assembly

Operational Temperature, °K (°F)	523 (482)
Operational Pressure, MPa (psia)	0.1075 (15.6)
Mixture Flow Rate, kg/hr (lb/hr)	1.314 (2.897)
ΔP across bed, cm H_2O	1.4

b) N_2O Decomposition Reactor Assembly

Operational Temperature, °K (°F)	723 (842)
Operational Pressure, MPa (psia)	0.1013 (14.7)
Mixture Flow Rate, kg/hr (lb/hr)	0.0194 (0.0428)
ΔP across bed, cm H_2O	1

$$h_o D_c/k = 0.6\ N_{Re}^{0.5}\ N_{Pr}^{0.31*}\ ,\ \text{for}\ 50 < N_{Re} < 10000 \qquad (1)$$

The heat-transfer coefficient of the fluid flowing inside the coil, based on the inside diameter, h_i, can be obtained using a method for a straight tube, such as a plot of the Colburn factor, j_h, versus Reynolds number. That must then be corrected for a coiled tube as follows:

$$h_{ic} = h_i\ [\ 1 + 3.5\ (D/D_H)\ ] \qquad (2)$$

The area needed for heat transfer is determined from the heat load and the log-mean-temperature-difference. The temperature difference is corrected to take into account the fact that the fluids are flowing perpendicular to each other.

The pressure drop inside the coil and in the annulus is obtained from the fluid flow equation:

$$\Delta P/L = 32\ f\ W^2\ /\ \pi^2\ \rho\ g_c D^5 \qquad (3)$$

The Fanning factor, f, is defined by the Colebrook equation:

$$1/\sqrt{f} = -4\ \log\ [(\varepsilon/44.4\ D) + (1.255/N_{Re}\ \sqrt{f}\ )] \qquad (4)$$

where is the pipe roughness. Pressure drops due to the joints, valves and sudden expansion and contraction were calculated from the tabulated values of friction-loss factors of each obstacle. The calculated sizes and geometries of the NH_3-oxidation and N_2O-decomposition assemblies are presented in Table 8.

Condenser.- The heat of condensation is the major source of energy in the catalytic water recovery process. This energy should be utilized in a proper condenser assembly to heat the urine recycle stream to the evaporation temperature. The condenser should also be capable of condensing

* The nomenclature of constants and other terms used in equations is presented on page 4 of this report.

TABLE 8

DESIGN DIMENSIONS OF THE REACTOR/HEAT EXCHANGER ASSEMBLIES

a) NH_3 Oxidation Reactor Assembly

Inside Diameter of the Reactor, cm	4.8
Outside Diameter of the Reactor, cm	5.1
Volume of Catalyst, cm^3	220
Bed Depth, cm	13.2
Inside Diameter of the Coil, cm	1.1
Outside Diameter of the Coil, cm	1.3
Length of the Helical Coil, cm	548.6
Number of Turns of Coil	23
Coil Pitch, cm	1.9
Helix Height, cm	44.9
Pressure Drop Inside the Coil, cm H_2O	2.5

b) N_2O Decomposition Reactor Assembly

Inside Diameter of the Reactor, cm	2.5
Outside Diameter of the Reactor, cm	5.4
Volume of Catalyst, cm^3	55
Bed Depth, cm	9.6
Inside Diameter of the Coil, cm	0.5
Outside Diameter of the Coil, cm	0.6
Length of the Helical Coil, cm	18.2
Number of Turns of Coil	14
Coil Pitch, cm	0.9
Helix Height, cm	14.0
Pressure Drop Inside the Coil, cm H_2O	0.35

water vapor in the presence of noncondensable gases and separating the recovered water from the gas phase. Based on previous experience, a concept utilizing a porous tube for condensing the recovered water was found to be the most suitable for this purpose.

In a condenser, the rate of condensation from a saturated mixture of vapor and noncondensable gas is governed primarily by the thermal resistance of the interface between the vapor-gas phase and the condensate film. Furthermore, condensation from a vapor-gas mixture does not occur at a nearly constant temperature as in the case of pure vapor. Instead, due to the change in the mass ratio of vapor and non-condensable gases, the temperature decreases as the mixture progresses through the condenser. When a vapor-gas mixture is fed to a condenser and the temperature of the condenser surface is below the dew point, a film of condensate forms on the surface and a film of non-condensable gas and vapor collects about it. In order for the vapor in the gas body to continue condensing into the condensate film, it must be driven across the gas film by the difference between the partial pressure of the vapor in the gas body and in the condensate. Therefore, the rate at which the steam condenses is no longer dependent entirely upon Nusselt's condensing mechanism but upon laws governing diffusion. When vapor diffuses through a gas film and liquifies at the surface, it also carrier with it its latent heat of condensation. In addition, there is also a temperature difference between the gas and the condensate film by which the gas sensibly cools. To accurately model this condensation process, it is necessary to use a stepwise numerical analysis, i.e., one in which the length of the condenser is divided into a series of finite elements. It is also necessary to consider the variation of local thermodynamic properties of the gas mixtures and their effect on the local heat and mass transfer coefficients for each finite element. One method of condenser design which satisfies the above requirement is the Colburn and Hougen technique. A three-man capacity tube and shell type condenser was designed by this technique using design factors summarized in Table 9.

Ranges of porous tube and jacket diameters were selected on the basis of the fluid velocity needed to provide high heat transfer rate combined with a low pressure drop. The required condenser surface area was then calculated for different combinations of diameters, and the optimum set was selected. The calculated dimensions were adjusted to convenient diameters of commercially available tubes, then the length required for obtaining the necessary surface area was calculated. Table 10 shows dimensions of the condenser components. The annulus and the tube side heat transfer coefficients were computed from the Sieder and Tate correlation. The mixture dew point along the condenser and the overall heat transfer coefficient were evaluated from the following heat balance:

$$h_i(T_g-T_c) + K_G M_v \lambda (P_v-P_c) = h_{oi} (T_c-T_w) = U (T_g-T_w) \qquad (5)$$

TABLE 9

DESIGN CONDITIONS FOR THE CONDENSER

Feed Rate	
Steam, kg/hr (lb/hr)	0.751 (1.65)
Non Condensables, kg/hr (lb/hr)	0.563 (1.24)
Condenser	
Inlet Temperature, °K (°F)	366.5 (200)
Outlet Temperature, °K (°F)	353 (176)
Pressure, MPa (psia)	0.107 (15.5)
Coolant Liquid	
Flow Rate, kg/hr (lb/hr)	52.2 (115.1)
Inlet Temperature, °K (°F)	348 (167)
Outlet Temperature, °K (°F)	353 (176)

TABLE 10

DESIGN DIMENSIONS OF THE CONDENSER

Porous Tube	
Inside Diameter, cm	1.9
Outside Diameter, cm	2.5
Length, cm	56.6
Inner Tube	
Inside Diameter, cm	2.8
Outside Diameter, cm	3.2
Outer Jacket	
Inside Diameter, cm	3.5
Outside Diameter, cm	3.8
Length, cm	57.1

To calculate the required surface area, the condenser was divided into a series of finite elements. The overall heat transfer coefficient and the dew point for each element were calculated from Equation 5. The area was calculated by numerically integrating the Newton equation.

The schematic of the condenser assembly is shown in Figure 10. The inner tube and the outer jacket are fabricated from standard size thin wall stainless steel tubing, and the porous tube is also seamless and commercially available. The coolant liquid is introduced tangetially and flows in the annular region between the inner tube and the outer jacket. The inlet and exit ports for the vapor-gas mixture are located at the two ends of the porous tube, and the mixture flows countercurrent to the coolant flow. A gap between the porous tube and the inner tube provides the passage for collecting the recovered condensate. To reduce the amount of heat losses, the condenser assembly is heavily insulated.

Evaporator.- A hollow fiber evaporator will be used in the system. Hot urine is circulated through the hollow fibers, while the outside surfaces of the fibers are exposed to a low partial pressure of water vapor, causing steam to evaporate. The heat of evaporation is provided by the hot urine flowing inside of the fibers.

The hollow fiber made from Nafion, a perfluoro-sulfonic acid ion-exchange material, is the prime choice. Permeability of these fibers for water vapor was estimated from the published experimental data of the TIMES water recovery unit. This value, corrected for our operating conditions, was used to calculate the membrane area. Changes in the membrane characteristic and water vapor pressure lowering in the recycle stream due to higher solid concentrations were considered in the design of the membrane evaporator. The permeability of the fibers and the pressure drop inside the fibers were calculated from the following equations:

$$JA = \frac{2\pi LNK(P_1 - P_2)}{\ln d_o/d_i} \tag{6}$$

$$\frac{\Delta P}{L} = 32\ f\ W^2\ /\ N\pi^2\rho g_c d_i \tag{7}$$

The evaporator operating conditions and the design dimensions are summarized in Tables 11 and 12. Figure 11 shows the schematic of the evaporator. The hollow fibers will be manifolded together into several bundles by connector headers made of silicone rubber or other suitable material. The bundles will be bonded in a cylindrical thin wall stainless

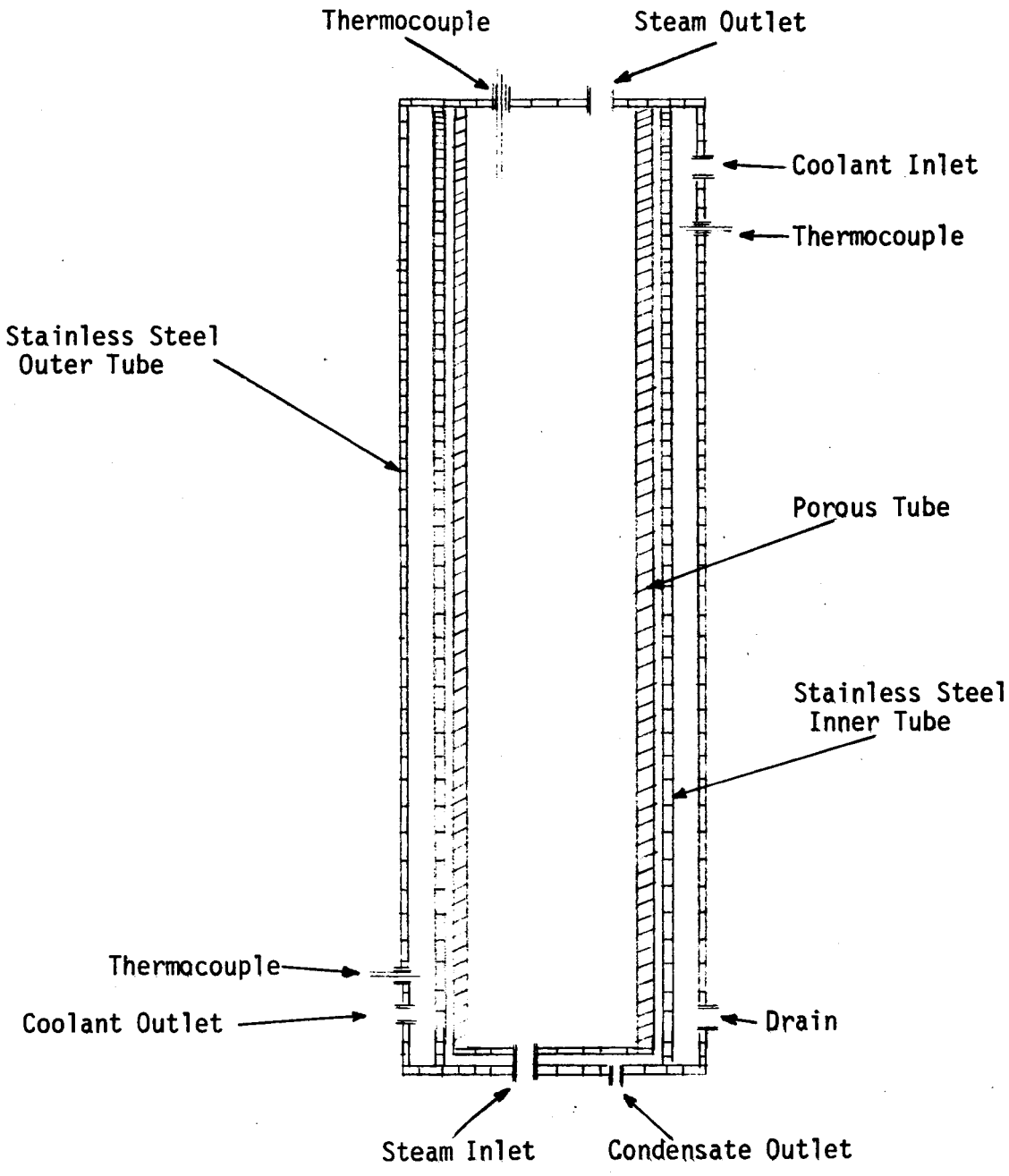

Figure 10 SCHEMATIC OF THE CONDENSER

TABLE 11

DESIGN CONDITIONS FOR THE EVAPORATOR

Urine	
Flow rate, kg/hr (lb/hr)	52.2 (115.1)
Inlet Temperature, °K (°F)	354 (178)
Outlet Temperature, °K (°F)	348 (167)
Vapor	
Flow rate, kg/hr (lb/hr)	0.551 (1.21)
Temperature, °K (°F)	343 (158)

TABLE 12

DESIGN DIMENSIONS FOR THE EVAPORATOR

Fiber	
Inside Diameter, mm	0.625
Outside Diameter, mm	0.875
Length, mm	300
Number	1576
Shell	
Length, cm	30.5
Diameter, cm	22.8
Lower Section	
Length, cm	7.6
Diameter, cm	15.2

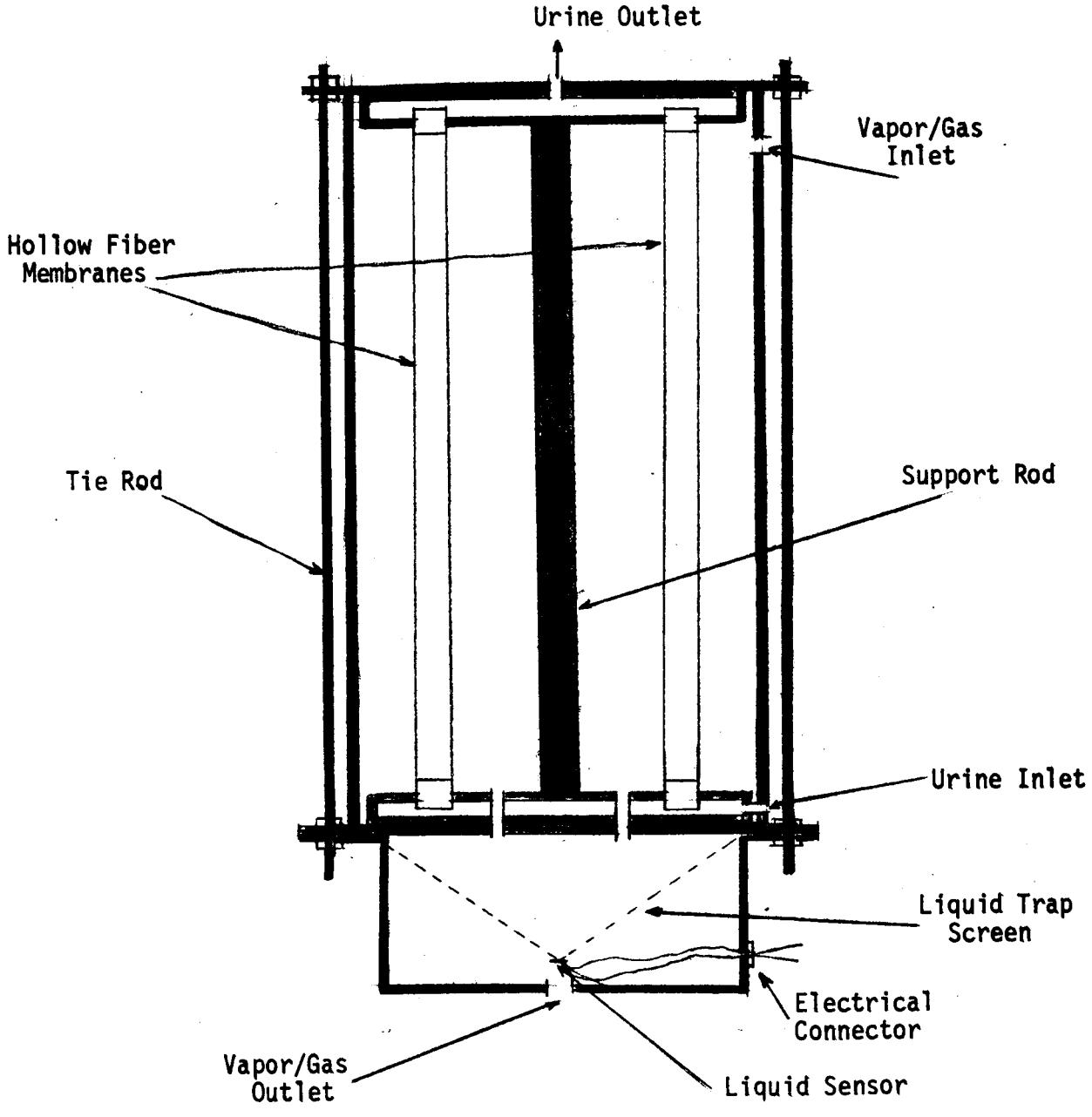

Figure 11 SCHEMATIC OF THE EVAPORATOR

steel cartridge assembly. The evaporator will be equipped with a liquid trap to trap any liquid breakthrough that might exist from a failed membrane condition and a sensor to signal the breakthrough of liquid. The liquid trap will be a hydrophobic screen that allows steam to flow through it and retains the liquid. The liquid trap and sensor will be easily removable from the assembly for maintenance and/or repairs.

Feed Heat Exchangers.- There are two feed streams entering the system: urine and oxygen. The urine feed will be preheated by the product water, and the oxygen feed will be preheated by the hot gas mixture leaving the nitrous oxide decomposition reactor. Due to the low flow rates and small heat transfer areas required for these feed streams, a double pipe heat exchanger shown in Figure 12 is a suitable choice. In the urine feed heat exchanger, urine flows inside the inner tube and the condensed water flows in the annular region between the inner and the outer tubes. In the oxygen feed exchanger, the gas mixture flows inside the inner tube and oxygen flows in the annular region. The principal parts of this kind of heat exchangers are two sets of concentric tubes, four connecting tees and a return bend. The inner pipe is supported within the outer pipe by packing glands and the fluid enters the inner pipe through a connection located outside the exchanger section. The tees are connected together to permit the entry and exit of the annulus fluid which crosses from one leg to the other through a return head. The two lengths of inner pipe are connected by a return bend which is exposed and does not provide heat transfer surface.

Double pipe heat exchangers were designed for the urine and oxygen feeds using design factors summarized in Tables 13 and 14. The heat transfer coefficients were obtained from the following equation:

$$h_i D/k = 1.86 \left[(N_{Re})(N_{Pr})(D/L) \right]^{1/3} \qquad (8)$$

The calculation consists of computing the heat transfer coefficient from the above equation and obtaining the surface area from the Fourier equation. The calculated dimensions of the heat exchangers are shown in Tables 15 and 16.

Recycle Tank.- After leaving the condenser, the recycling urine will be further heated by the hot vapor/gas mixture leaving the NH_3 oxidation reactor, using an appropriate heating loop built in the recycle tank. A heater will be installed in the tank for preheating the recycle fluid during start-up.

The heat transfer coefficient for the tube side was calculated from equation (1), and it was corrected for a coiled tube by equation (2). The shell side coefficient was determined from equation (8) by substituting

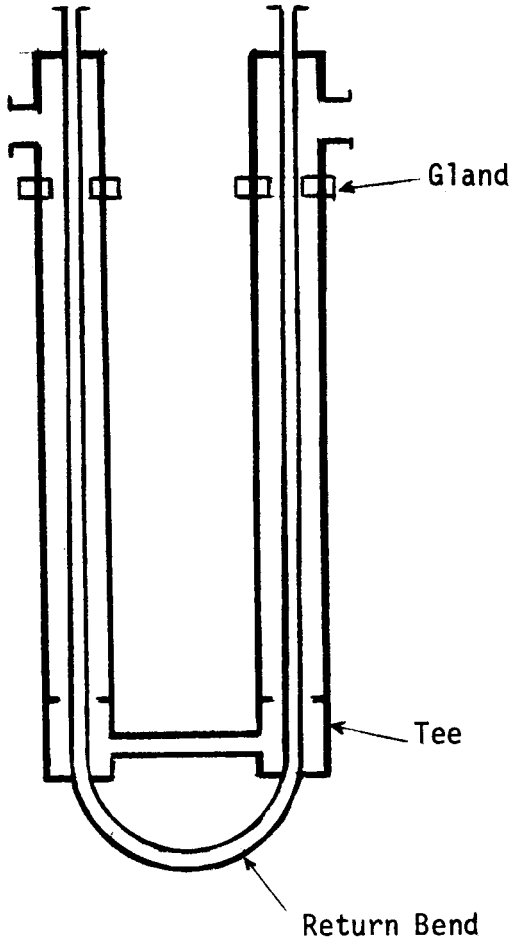

Figure 12 SCHEMATIC OF A DOUBLE PIPE HEAT EXCHANGER

TABLE 13

DESIGN CONDITIONS FOR THE
URINE FEED HEAT EXCHANGER

Flow Rate	
Urine, kg/hr (lb/hr)	0.587 (1.29)
Water, kg/hr (lb/hr)	0.546 (1.20)
Inlet Temperature	
Urine, °K (°F)	298 (77)
Water, °K (°F)	353 (176)
Outlet Temperature	
Urine, °K (°F)	333 (140)
Water, °K (°F)	308 (95)

TABLE 14

DESIGN CONDITIONS FOR THE
OXYGEN FEED HEAT EXCHANGER

Flow Rate	
Oxygen, kg/hr (lb/hr)	0.027 (0.059)
Vapor/gas, kg/hr (lb/hr)	0.019 (0.042)
Inlet Temperature	
Oxygen, °K (°F)	298 (77)
Vapor/gas, °K (°F)	373 (212)
Outlet Temperature	
Oxygen, °K (°F)	353 (176)
Vapor/gas, °K (°F)	308 (95)

TABLE 15

DESIGN DIMENSIONS OF THE
URINE FEED HEAT EXCHANGER

Inner Tube	
Inside Diameter, cm	0.33
Outside Diameter, cm	0.47
Outer Tube	
Inside Diameter, cm	0.65
Outside Diameter, cm	80.74
Tube Length, cm	126.5

TABLE 16

DESIGN DIMENSIONS OF THE
OXYGEN FEED HEAT EXCHANGER

Inner Tube	
Inside Diameter, cm	0.33
Outside Diameter, cm	0.48
Outer Tube	
Inside Diameter, cm	0.62
Outside Diameter, cm	0.79
Tube Length, cm	33.3

the equivalent diameter D_e for D. The equivalent diameter was obtained by calculating the non occupied volume of the vessel V_f, and using the following equation:

$$D_e = \frac{4V_f}{\pi d_o L} \tag{9}$$

The schematic of the recycle tank is shown in Figure 13; it will be fabricated from thin-walled stainless steel tubing.

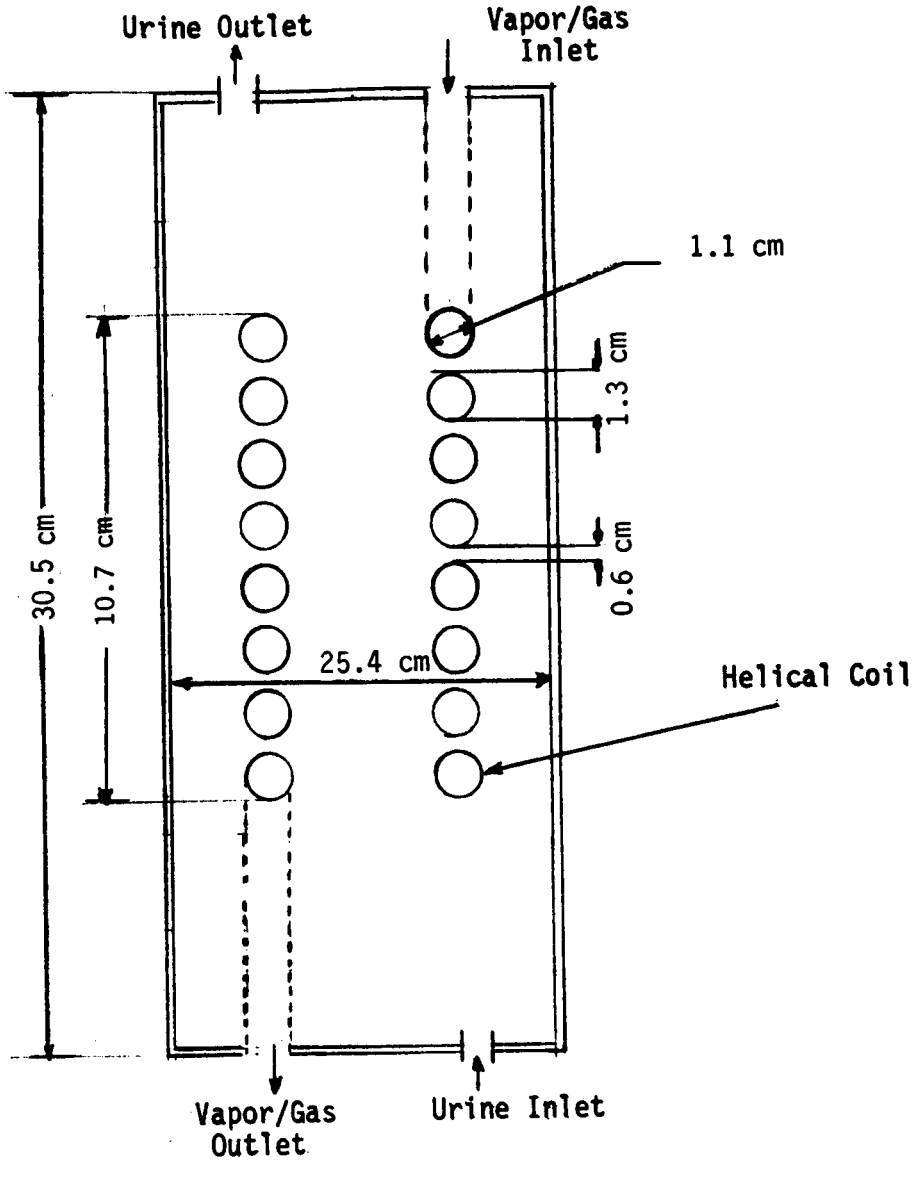

Figure 13 SCHEMATIC OF THE RECYCLE TANK

FABRICATION

The basic components of the subsystem are the two catalytic reactors, evaporator, condenser, urine recycle tank and the heat exchangers. The fabrication of all the components was based on the design concept and calculated dimensions; however, since commercially available thin-wall #304 stainless steel tubing was used, the design dimensions were slightly adjusted to conform to standard tubing sizes.

Ammonia Oxidation Reactor

Figures 14 and 15 show the schematic cutaway and cross sectional views of the ammonia oxidation reactor; Figures 16, 17, 18 and 19 show the actual components, their arrangement and the completed reactor.

A Fire rod cartridge heater (0.95 cm (3/8") O.D, 30.5 cm (12" long), 400 watts) situated in the center of the assembly and surrounded by a 1.27 cm (1/2") diameter heater housing tube is used for preheating the reactor during start-up and for maintaining the required operational temperature under the anticipated flow conditions. A catalyst bed consisting of 250g of 0.5% Pt on 0.32 cm (1/8") alumina pellets is placed in the annulus created by the heater housing tube and the reactor wall. The volume of this annulus is somewhat larger than the calculated volume of catalyst; thus, it can accommodate additional catalyst, if required. The catalyst bed is enclosed and supported by perforated plates at each end. A port was provided for introducing catalyst to the catalyst bed. Initially three thermocouples, one at each end and in the center of the catalyst bed, were installed for measuring and controlling the temperature. But during the system testing, a leak was detected in the thermocouple well, thus one of the thermocouples was removed and its well was permanently sealed. A heat exchanger coil for preheating the feed with the product stream surrounds the reactor and is enclosed by the outside tube. Two thermocouples are installed in the annulus to measure the inlet and the outlet temperatures of the gas stream to the annulus. The entire assembly was thermally insulated by blanket type, high temperature insulation to minimize heat losses to the atmosphere.

The gas/vapor mixture from the compressor enters the heat exchanger coil at the top of the reactor and is preheated by the outgoing stream. The mixture then flows inside the annulus between the heater and its housing and is further heated to the desired temperature. The hot gas/vapor mixture passes through the catalyst bed and is directed to the annulus surrounding the heat exchanger coil through the holes at the lower section of the assembly and flows through the annulus preheating the feed flowing inside the coil and leaving the reactor assembly at the other end.

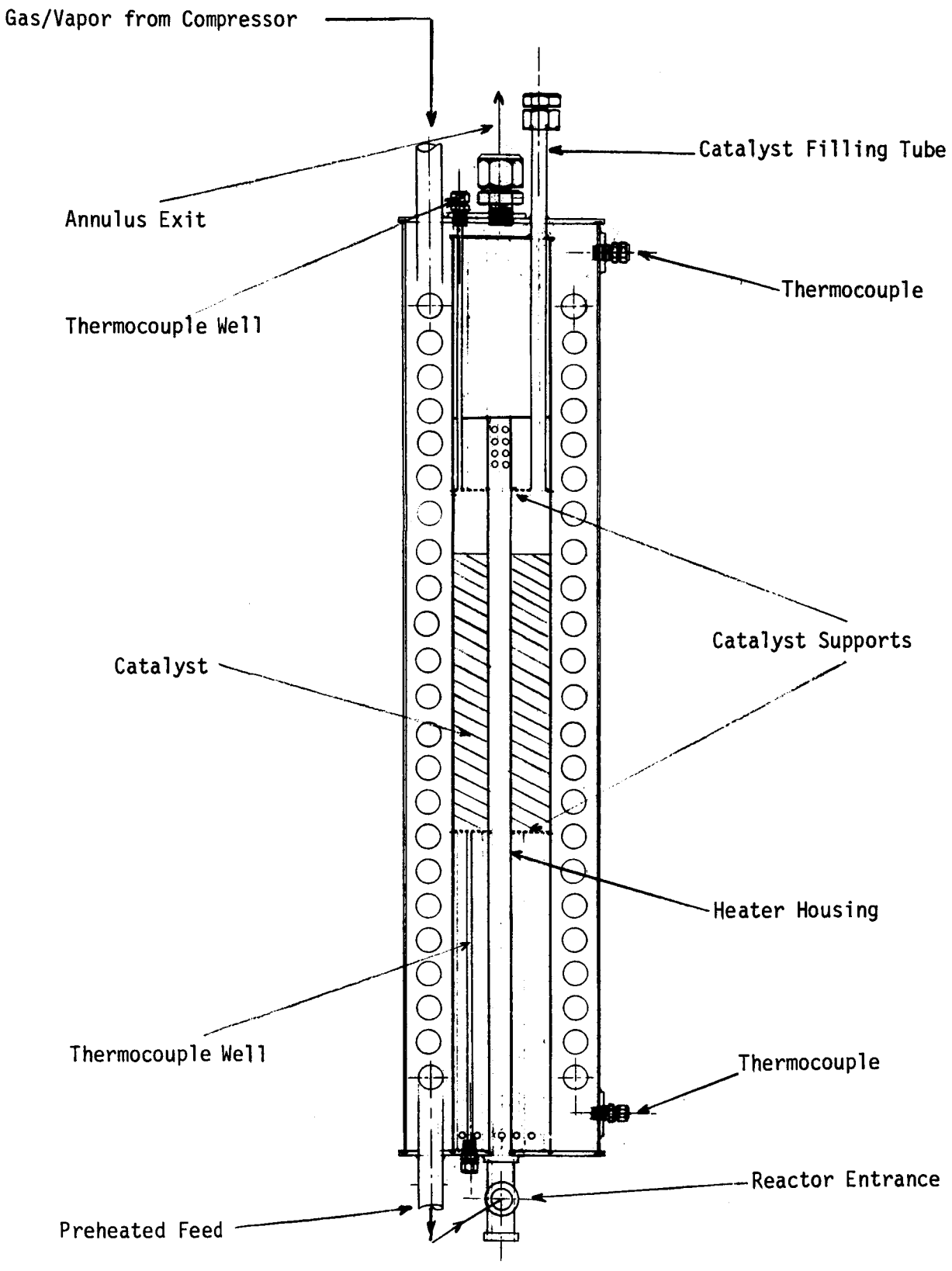

Figure 14 CUTAWAY VIEW OF THE REACTOR/HEAT EXCHANGER

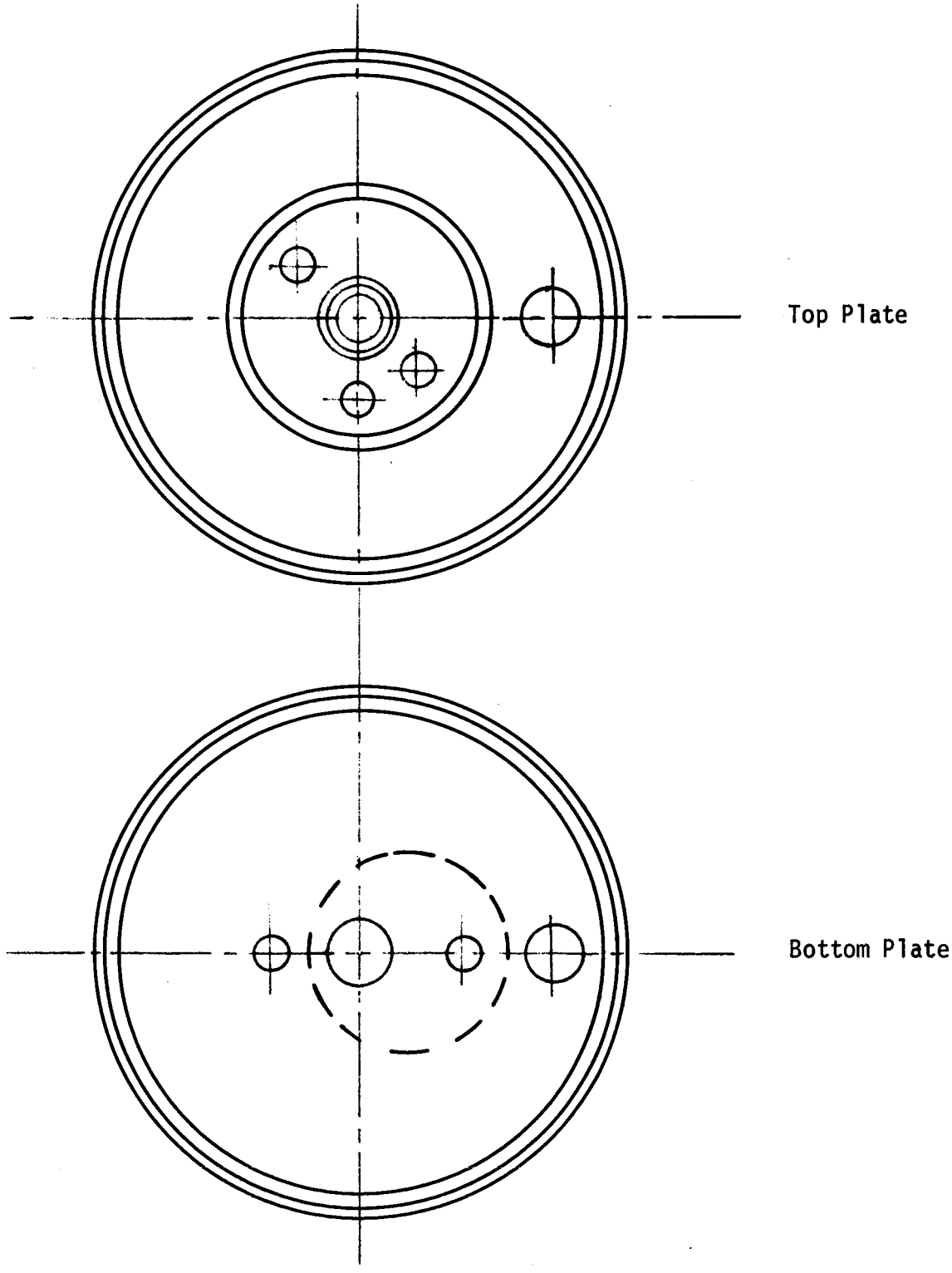

Figure 15 CROSS SECTIONAL VIEWS OF THE END-PLATES

Figure 16 COMPONENTS OF THE AMMONIA OXIDATION REACTOR/HEAT EXCHANGER

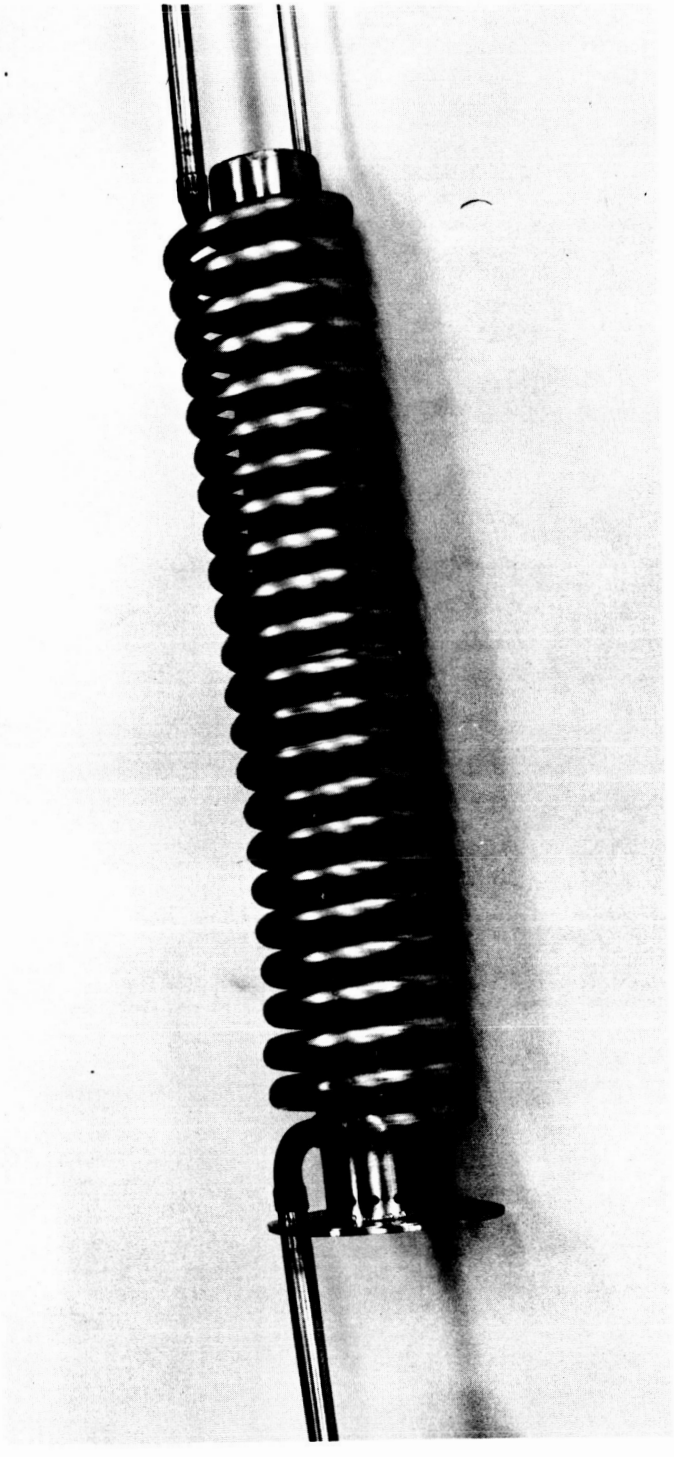

Figure 17 PARTIALLY ASSEMBLED REACTOR/HEAT EXCHANGER

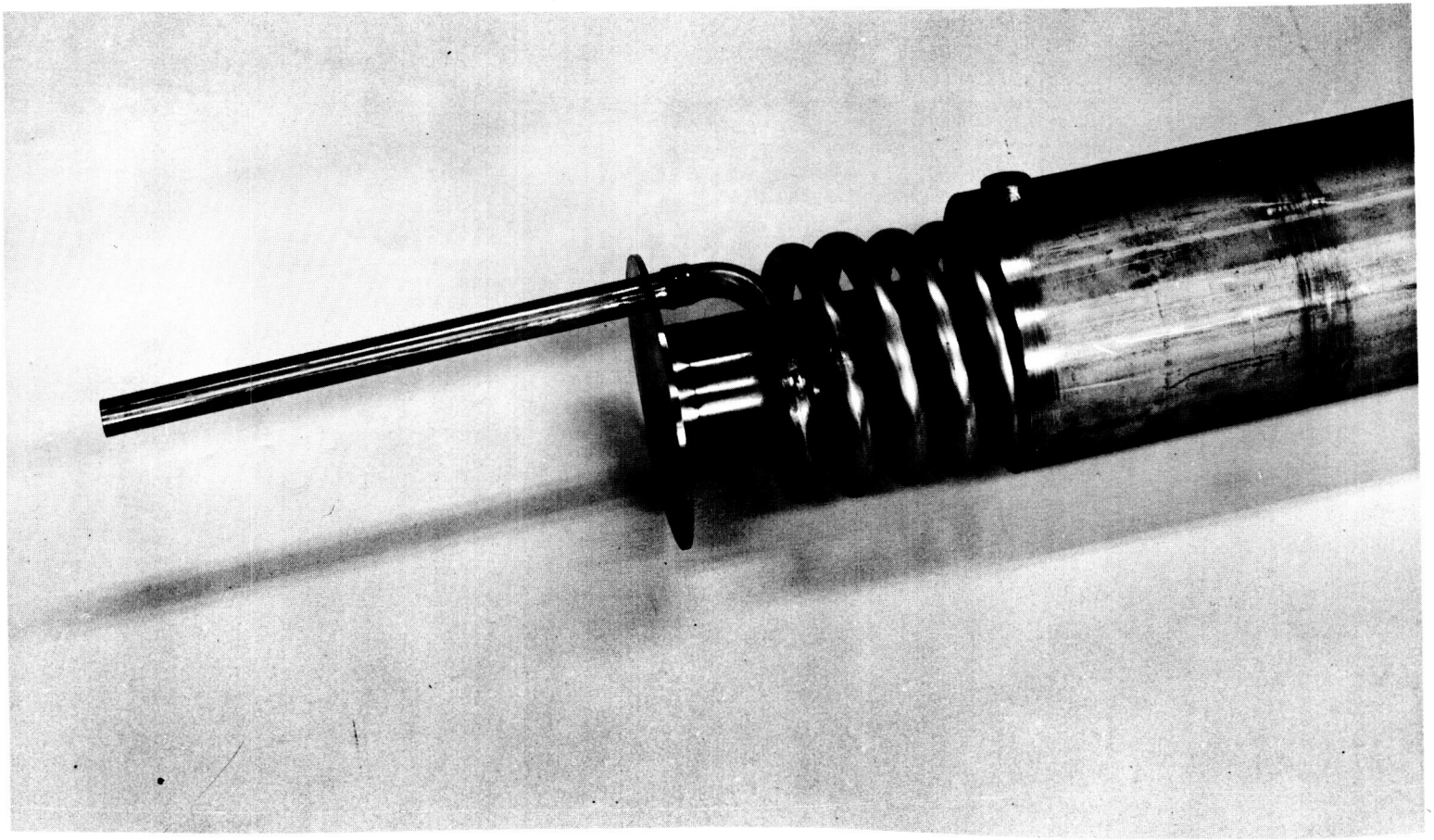

Figure 18 FINAL ASSEMBLY OF REACTOR/HEAT EXCHANGER

ORIGINAL PAGE IS
OF POOR QUALITY

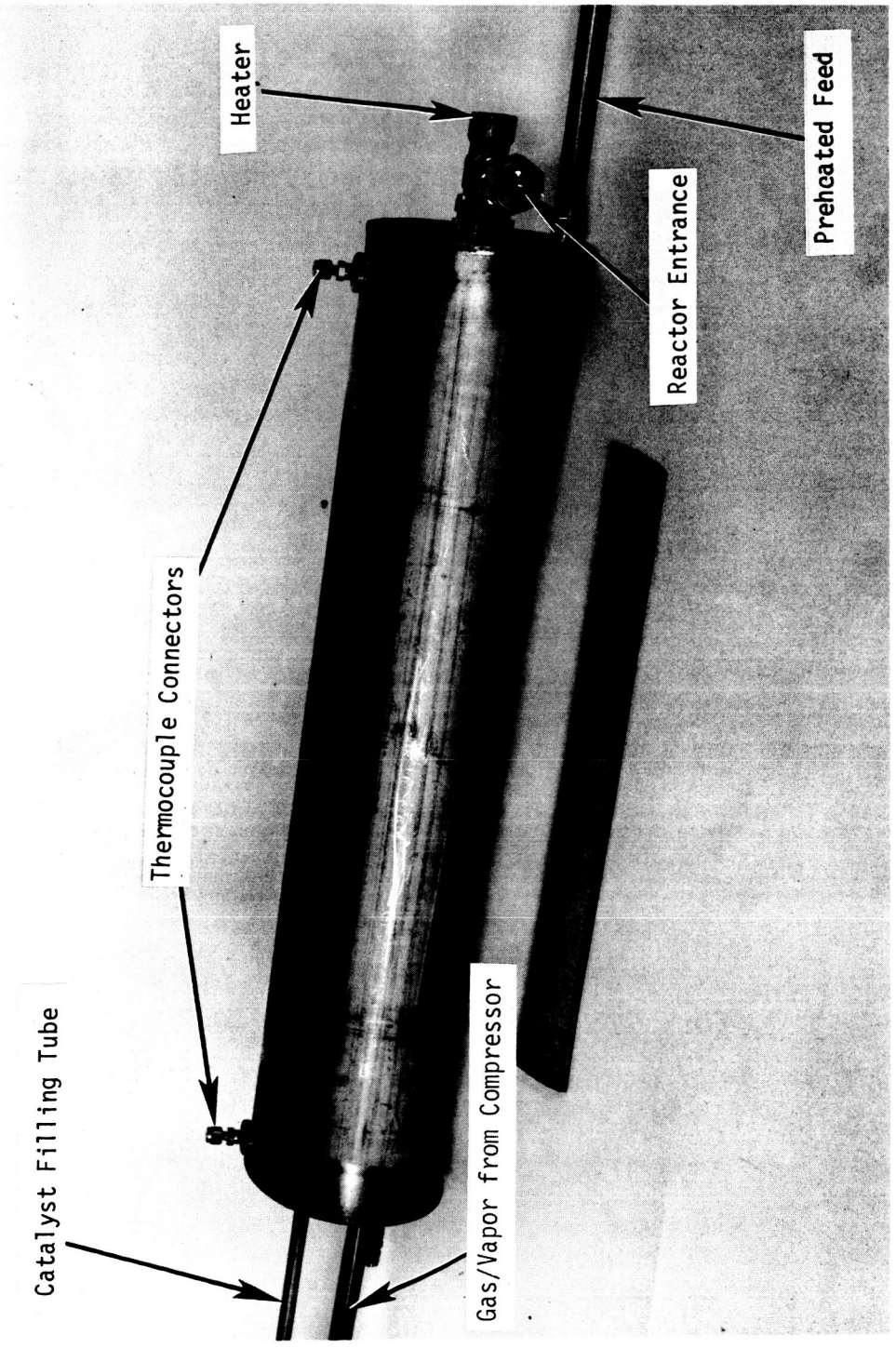

Figure 19 ASSEMBLED REACTOR/HEAT EXCHANGER

N_2O Decomposition Reactor

The initial design considered an N_2O decomposition reactor similar to the NH_3 oxidation reactor. Testing, however, indicated that the flowrate was too low for achieving any meaningful heat transfer in the heat exchanger and, in fact, the entire assembly adjusted itself to one overall temperature. Thus, the design was changed to a simple heated flow-through reactor, shown in Figure 20.

The reactor is fabricated from stainless steel tubing (2.2 cm (0.87") ID, 2.54 cm (1") OD, 12.7 cm (5") long). A cartridge heater (1.27 cm (1/2"), 10.2 cm (4"), 100 watts) is installed in the center of the tube. The annulus created by the heater and the tube contains the catalyst bed which is enclosed and supported by perforated plates at each end. The reactor contains 49 g (0.32 cm (1/8")) catalyst pellets. A thermocouple is installed in the middle of the reactor to measure the bed temperature. The reactor is heavily insulated with high temperature insulation material.

Evaporator

The schematic cutaway of the evaporator is shown in Figure 21. The evaporator consists of three main parts: the container, the hollow fiber bundle holder and the fiber bundles. The container is fabricated from standard size (14.9 cm (5.87") ID, 15.2 cm (6") OD) thin-walled stainless steel tubing. At a 5 cm (2") distance from the bottom, a ring is welded inside the container to hold the bundle holder and a conical stainless steel screen which is coated with Teflon and contains liquid sensor electrodes installed at its apex. The screen covers the vapor exit openings for retaining liquid urine that may escape due to a failed membrane. The vapor/gas inlet and outlet connectors and thermocouple connectors are all installed on the container.

The bundle holder is also fabricated from stainless steel and consists of two headers connected to each other by three support rods. Six bored through Swagelok bolts are brazed to each header to provide connections for mounting the hollow fiber bundles to the assembly. The liquid entrance and exit to the evaporator and thermocouple connectors are located on top of the bundle holder. The bundle holder can be separated from the container for mounting the hollow fiber bundles. The bundle holder and the container are bolted together, and rubber gaskets are used at all joints to ensure good leak-tight seals. The evaporator was thermally insulated by blanket type insulation.

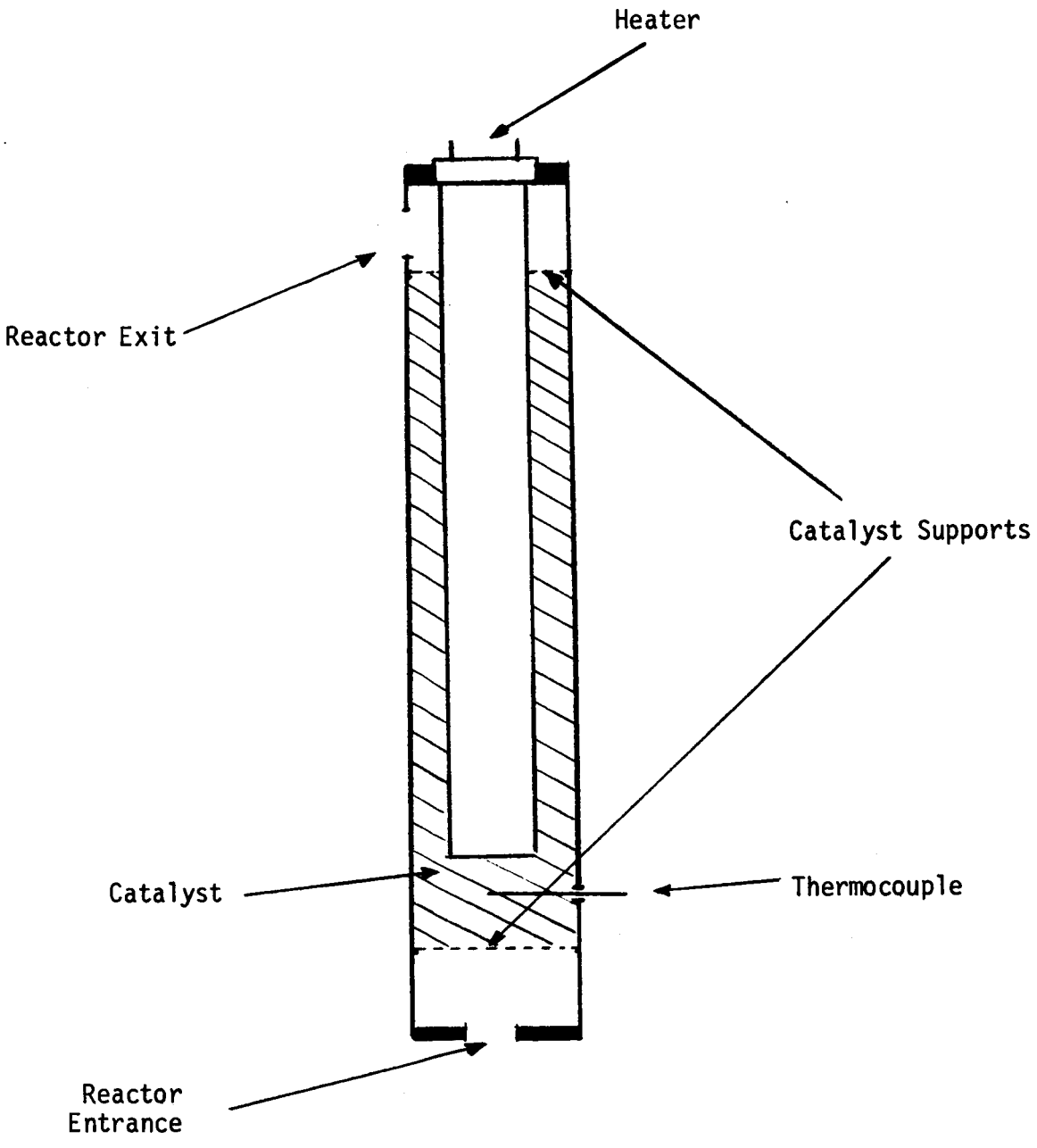

Figure 20 NITROUS OXIDE DECOMPOSITION REACTOR

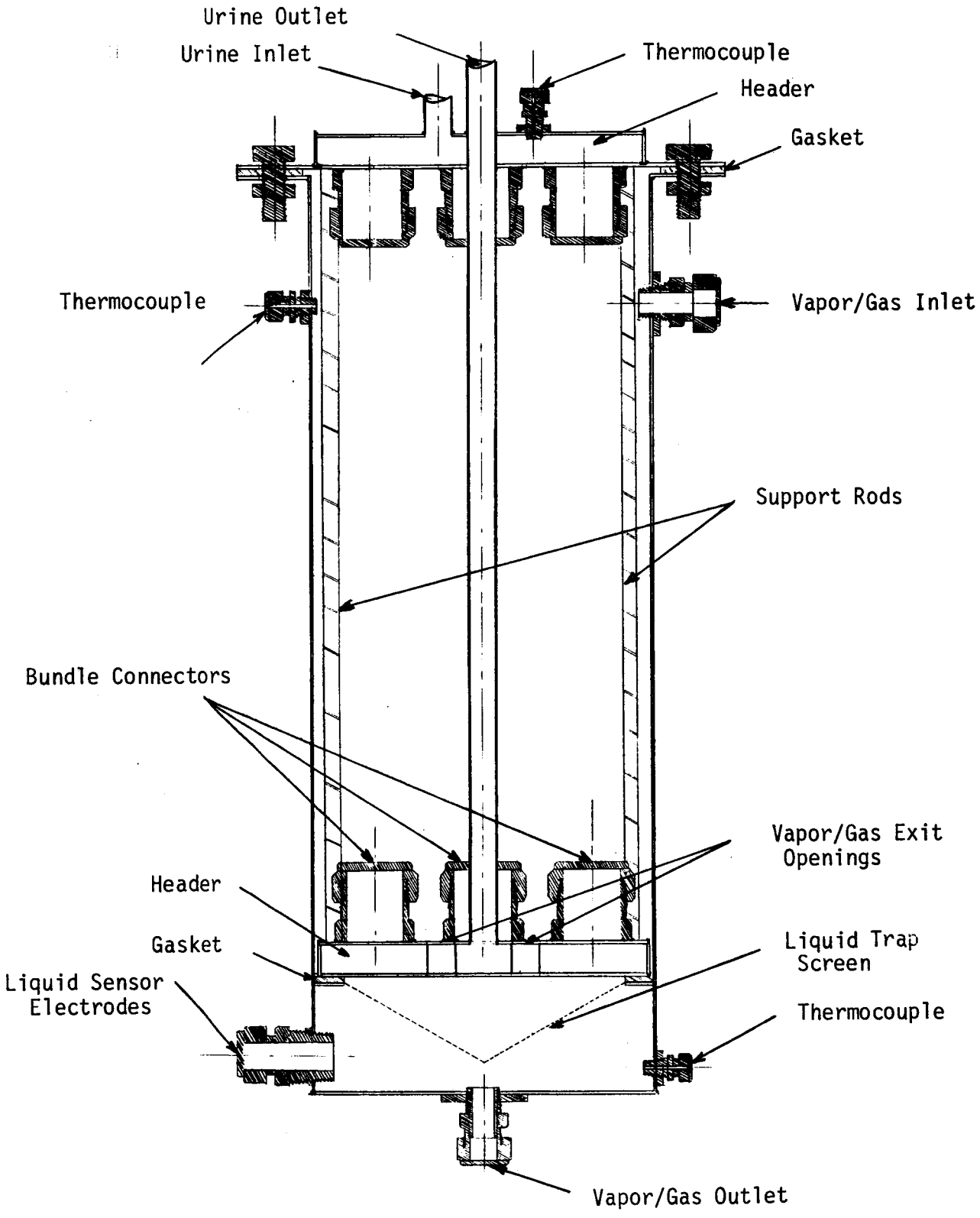

Figure 21 CUTAWAY VIEW OF THE EVAPORATOR

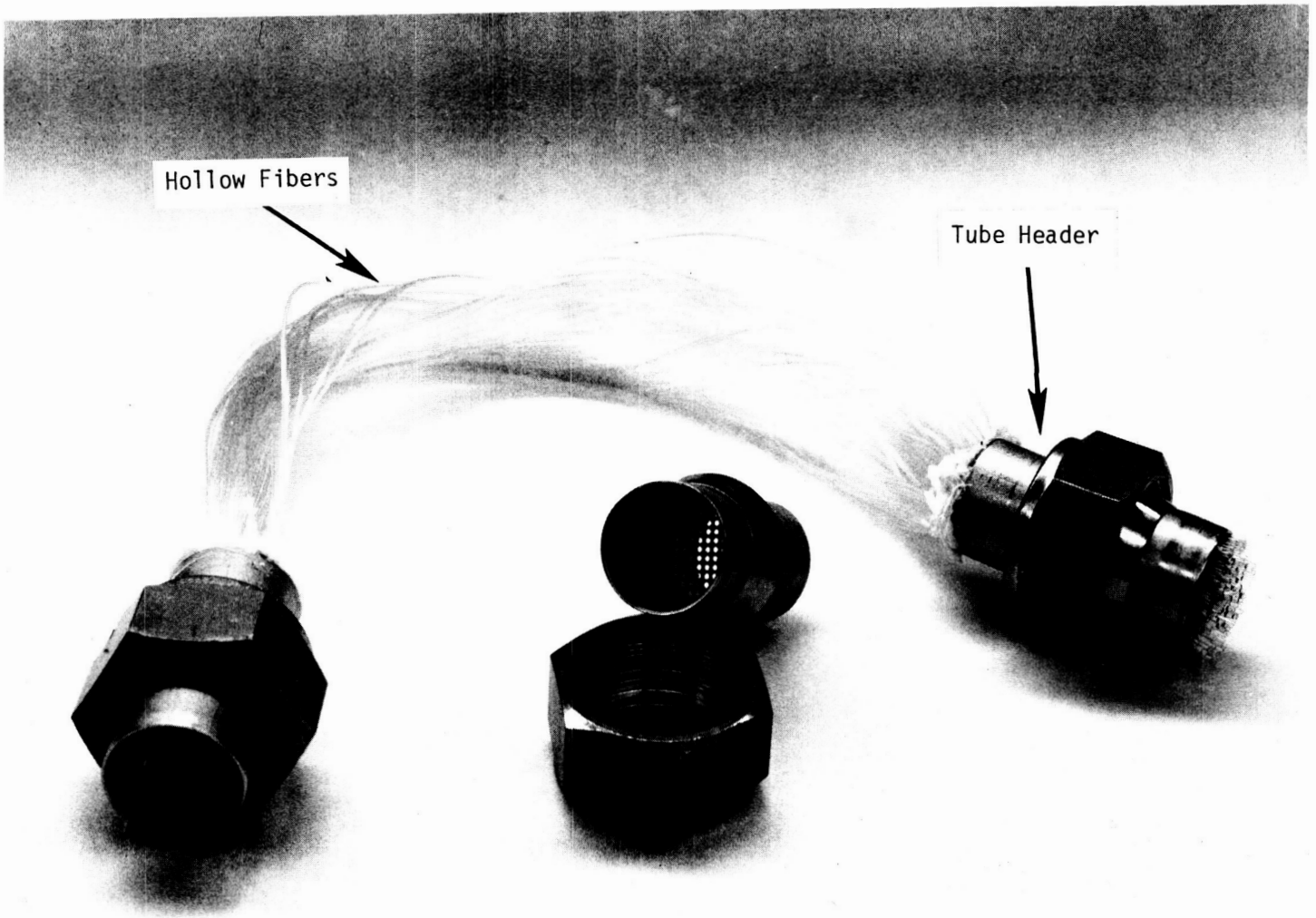

Figure 22 FIBER BUNDLE AND ITS COMPONENTS

Six hollow fiber bundles with total surface area of about 0.69 m^2 (7.4 ft^2) were prepared from Nafion (a perfluorinated ion exchange polymer) tubing (0.61 mm ID, 0.86 mm OD) obtained from Permapure Products. The individual fibers were manifolded together at each end by stainless steel tube headers. Each header was made by fastening a screen inside a 2.5 cm (1") OD, 5 cm (2") long stainless steel tubing at a 2 cm (0.75") distance from one end. The openings of the screen were only slightly larger than the diameter of the fiber to allow passage of the hollow fibers. The space between fibers inside the tube was filled with epoxy glue, providing a leak tight seal. A Swagelok nut and ferrules were tightened on each header to provide leak tight connections between the bundles and the bundle holders. Figure 22 shows the fiber bundle and its components. Three of the mounted bundles are shown in Figure 23. The sequence of the evaporator assembly is depicted in Figures 24, 25 and 26.

Heated urine enters the evaporator at the top of the assembly, flows downward through the hollow fiber membranes and leaves the evaporator through the central tube. The vapor/gas mixture from the recycle stream enters at the top of the evaporator and becomes enriched by the vapor permeating the wall of the hollow fibers. The vapor/gas mixture then passes through the liquid trap and leaves the evaporator at the bottom end of the assembly.

Condenser

The schematic of the condenser is shown in Figure 27. The inner tube and the outer jacket of the condenser are fabricated from stainless steel tubing (4.4 cm (1.74") ID, 4.7 cm (1.87") OD and 6.1 cm (2.4") ID, 6.3 cm (2.5") OD, respectively). The porous tube was constructed by rolling a 0.32 cm (0.125") thick porous copper sheet and silver brazing the sides together. Steam is introduced tangentially and flows in the annular region between the porous tube and the outer jacket. The inlet and exit ports for the urine are located at the two ends of the inner tube, and the urine flows countercurrent to the vapor/gas flow. A capiliary gap between the inner tube and the porous tube provides the passage for collecting the recovered condensate. Due to the higher than atmospheric pressure in the condenser, the condensate is pushed out automatically. The flow rate of the condensate is controlled by adjusting a metering valve located at the end of the recovery line. Connectors are provided on the outer jacket for thermocouples, pressure gauge and pressure relief valve. The condenser is heavily insulated by blanket type insulation material. Pictures of the actual components and assembly are shown in Figures 28, 29 and 30.

Urine Recycle Tank - The cutaway and the completed views of the urine recycle tank are shown in Figures 31 and 32. The recycle tank is

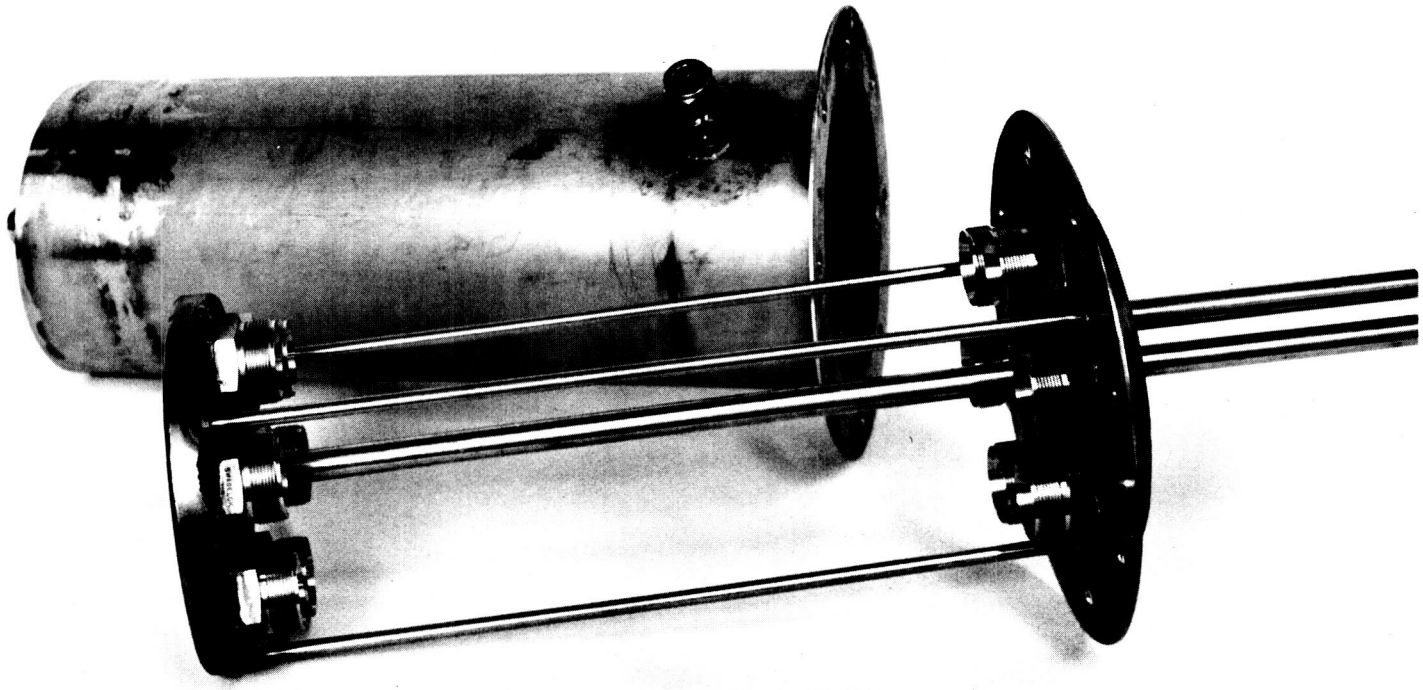

Figure 24 COMPONENTS OF THE EVAPORATOR

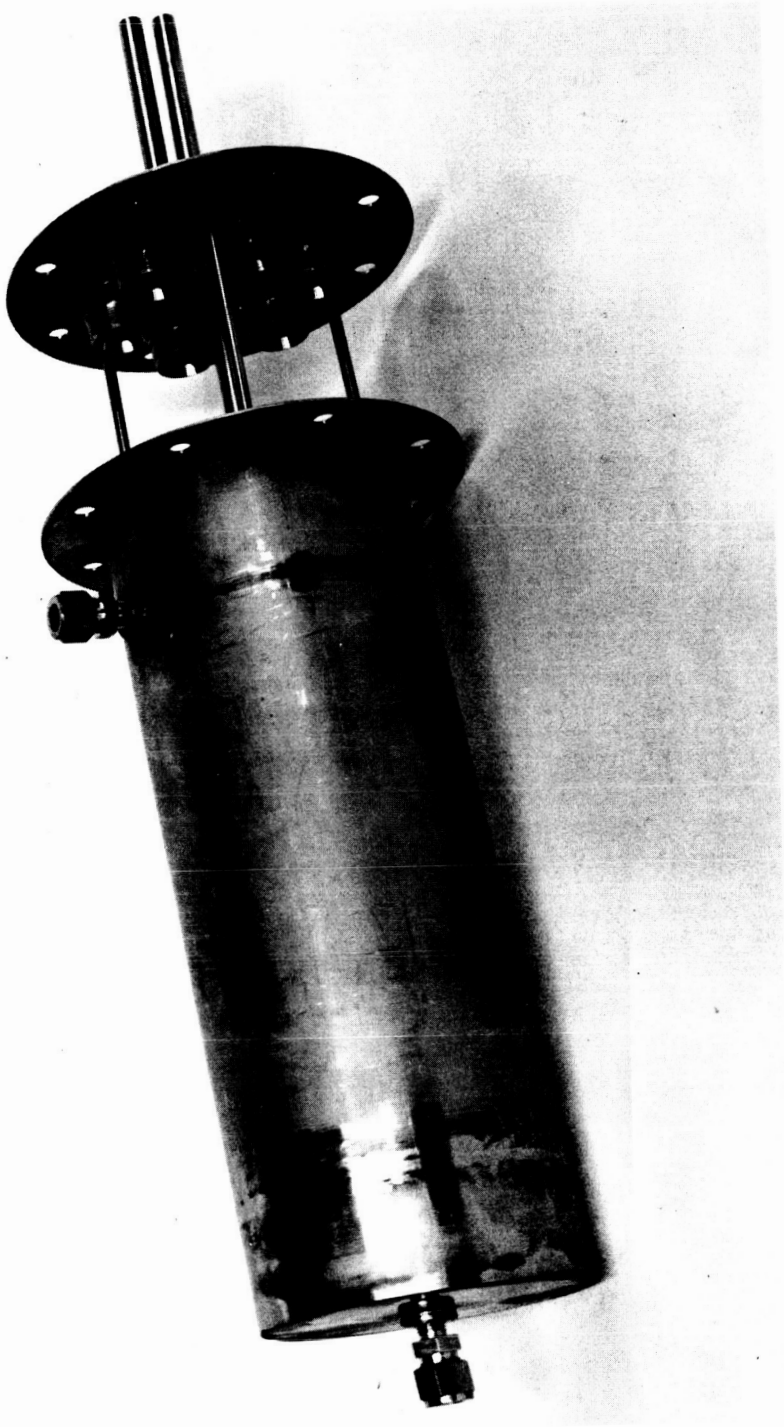

Figure 25 PARTIALLY ASSEMBLED EVAPORATOR

Figure 26 ASSEMBLED EVAPORATOR

Figure 26 ASSEMBLED EVAPORATOR

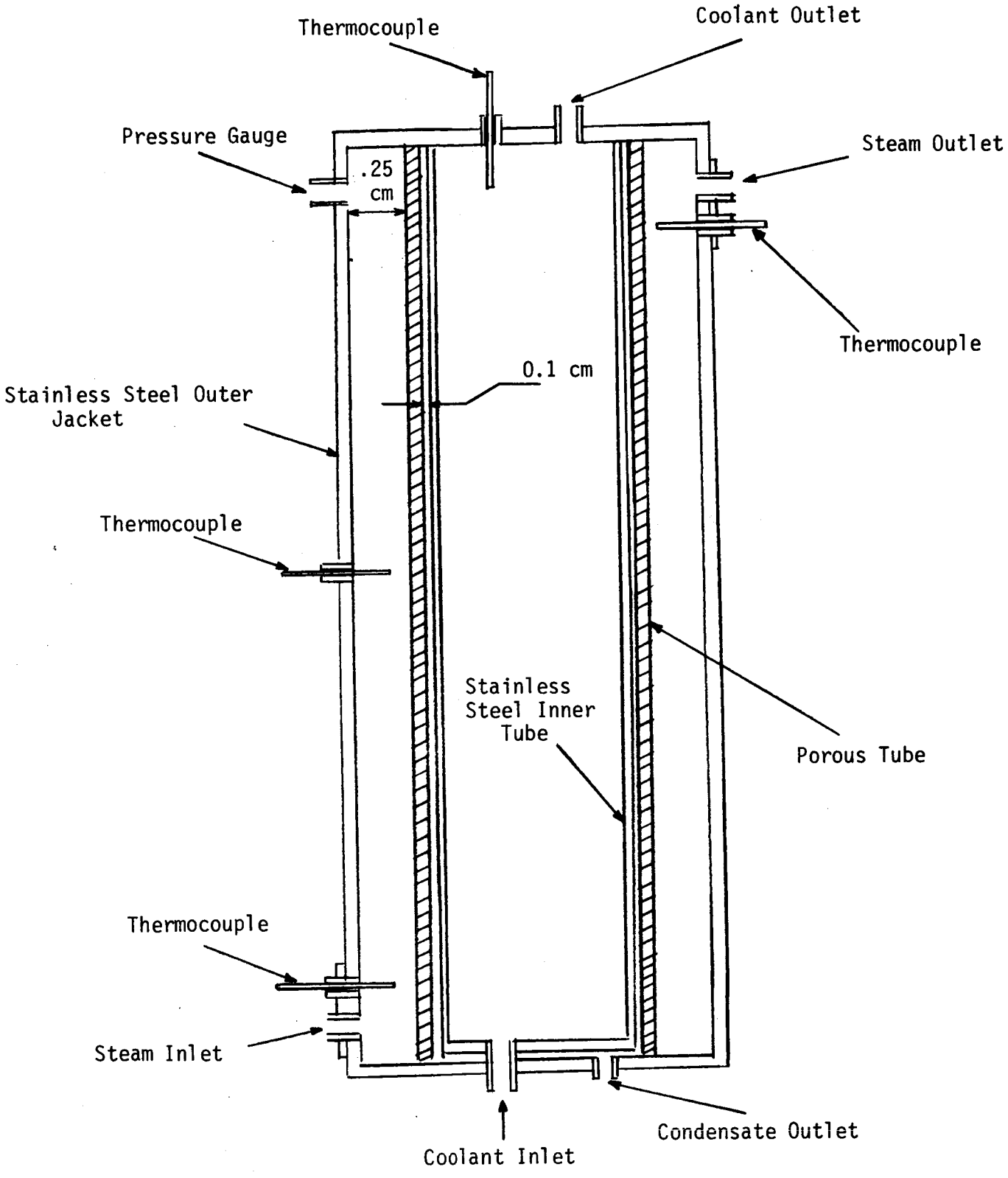

Figure 27 SCHEMATIC OF THE CYLINDRICAL CONDENSER

Figure 28 COMPONENTS OF THE CYLINDRICAL CONDENSER

Figure 29 CYLINDRICAL CONDENSER CROSS SECTION

ORIGINAL PAGE IS
OF POOR QUALITY

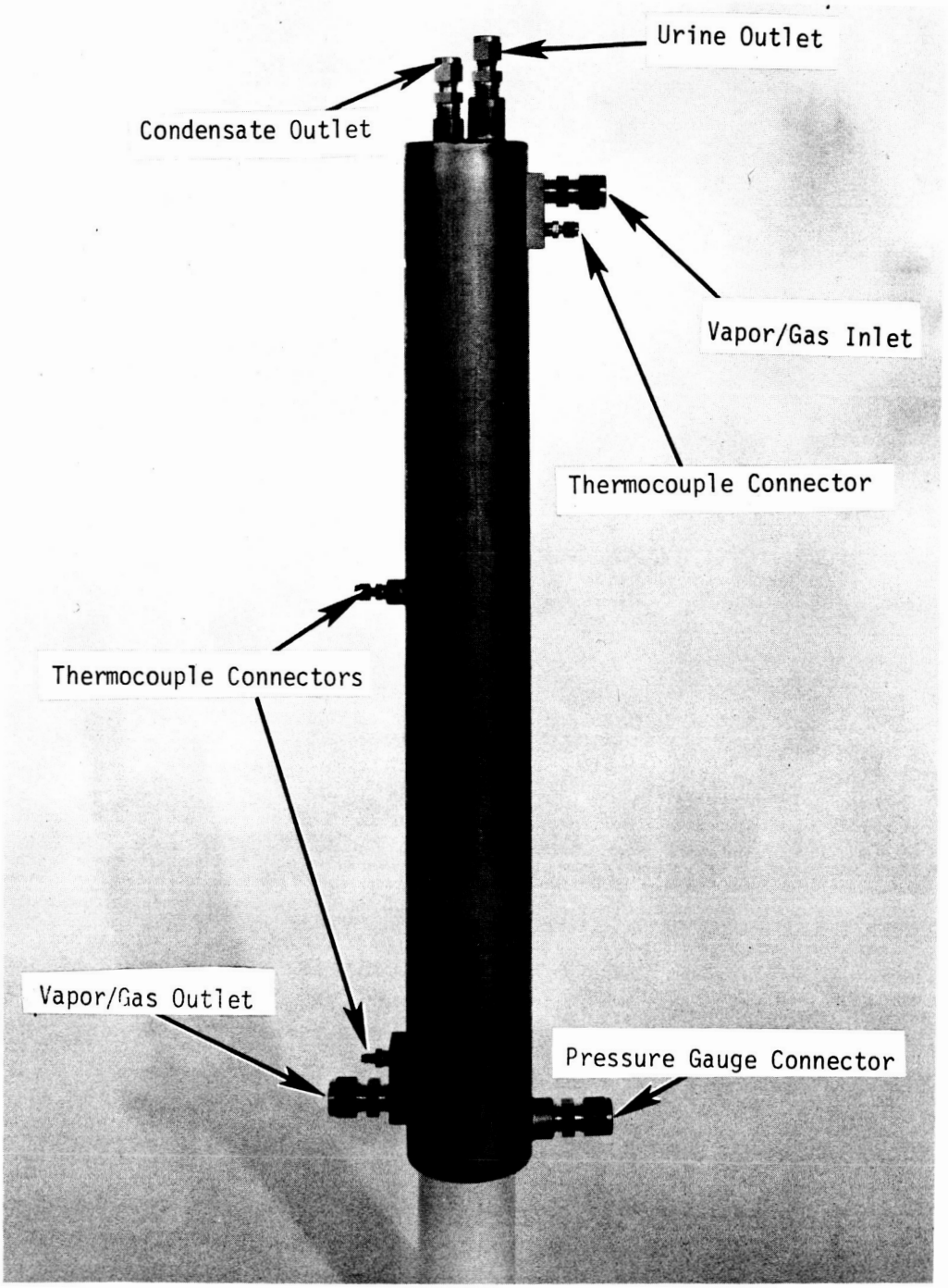

Figure 30 ASSEMBLED CYLINDRICAL CONDENSER

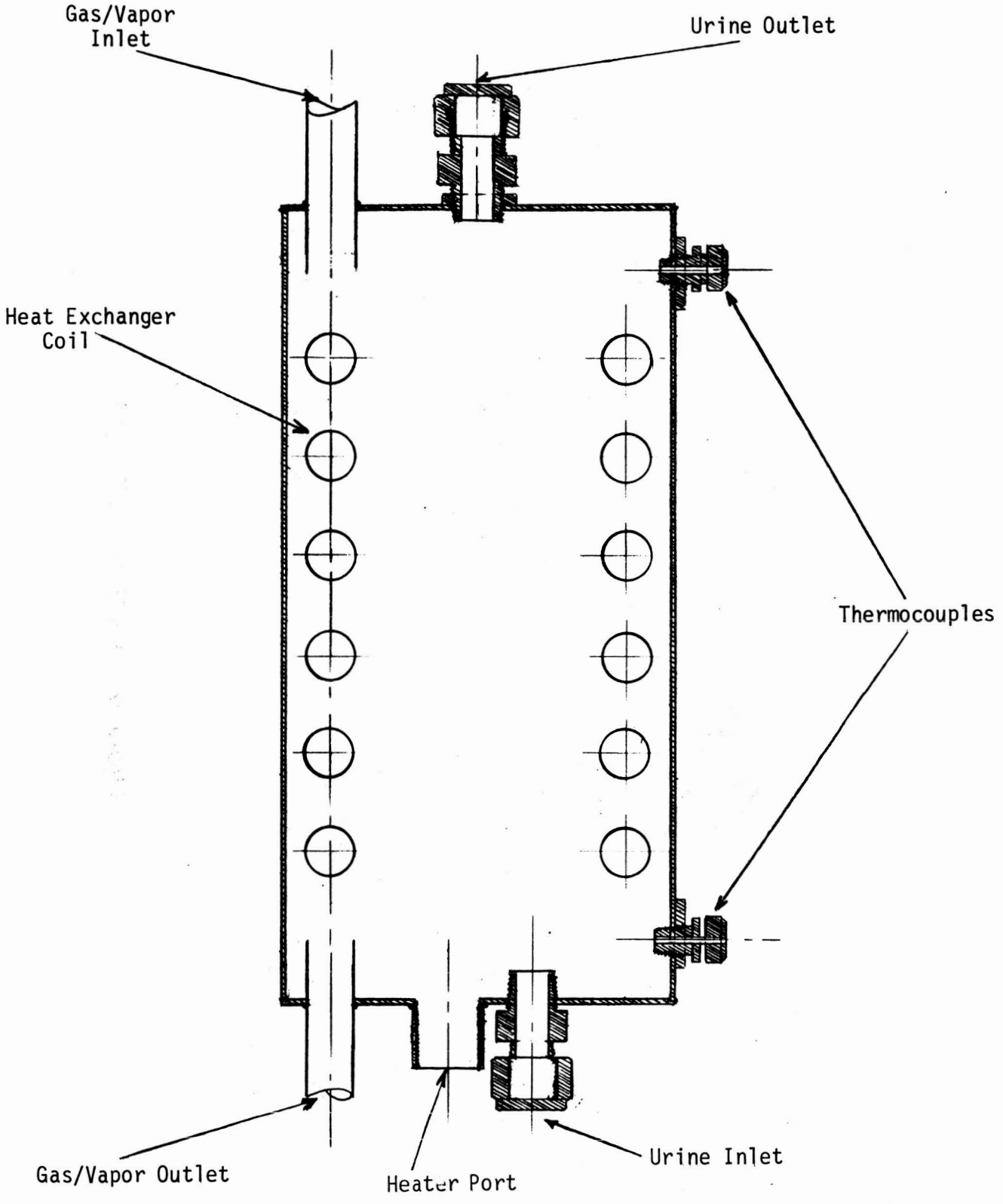

Figure 31 CUTAWAY VIEW OF THE RECYCLE TANK

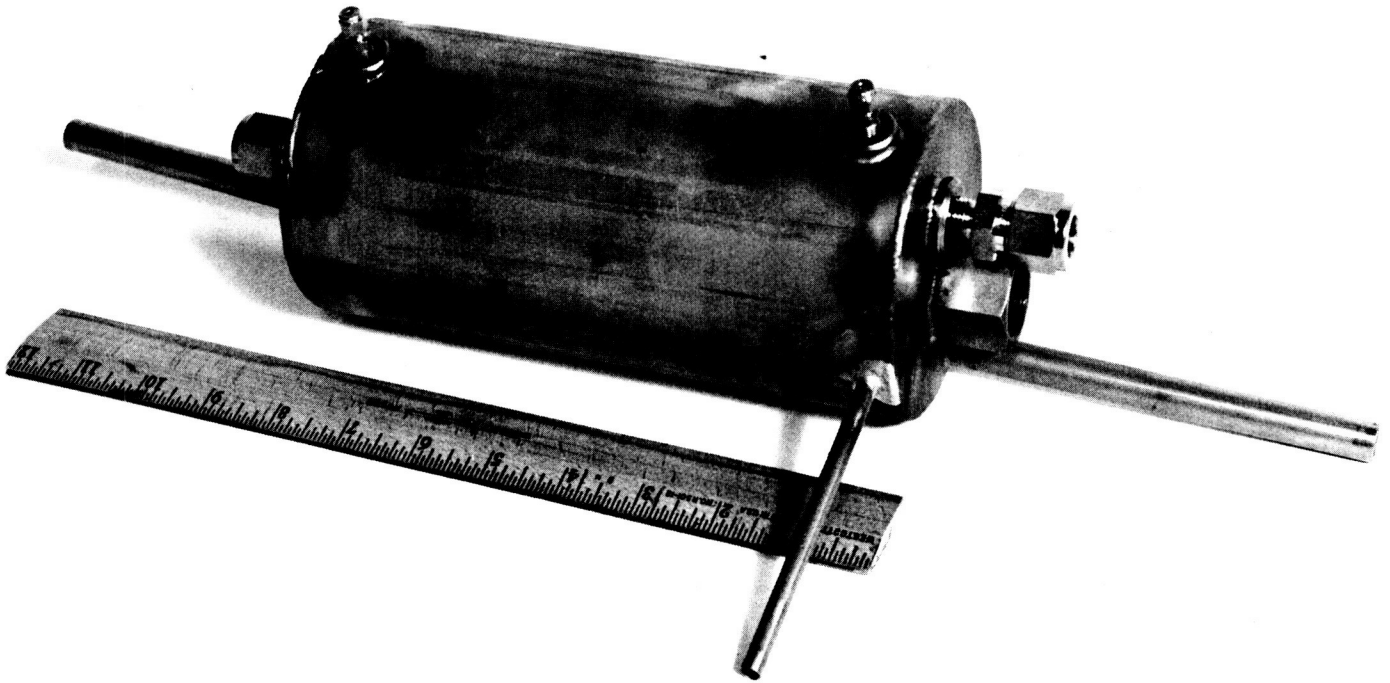

Figure 32 ASSEMBLED RECYCLE TANK

fabricated from stainless steel tubing (9.8 cm (3.87") ID, 10.1 cm (4") OD). A cartridge heater (0.95 cm (3/8") OD, 12.7 cm (5") long, 300 watts) situated in the center is used for preheating during the start-up and for maintaining the temperature during the run, as needed. Two thermocouples are installed for measuring and controlling the temperature of the urine. A heat exchanger coil is installed inside the tank for preheating the urine with the gas stream leaving the ammonia oxidation reactor. During start-up, urine bypasses the evaporator and enters the top of the recycle tank. The heated urine then leaves at the bottom of the tank and joins the recycling stream. During the run, the recycling urine passes through the evaporator and some portion of it follows the previous path through the recycle tank to maintain the desired temperature.

Blower/Compressor

The process requires a small blower/compressor for recirculating and compressing the vapor/gas mixture and for preheating the mixture by compression before entering the NH_3 oxidation reactor. In the selection of the compressor the following points were considered:

a) Commercial availability,
b) Low power requirement,
c) Capability to withstand high temperatures so that the compressor could be insulated and the heat of compression transfered to the process gas instead of being lost to the atmosphere,
d) High chemical resistivity,
e) Capability to compress wet vapors.

One type of compressor which is capable of compressing wet vapors without damage is screw type compressor. But the problem is that all the commercially available compressors of this type are too large for this application and do not meet other requirements.

In view of these problems, a bellows type blower which met most of the requirements was obtained from Metal Bellows Corporation. Two different versions of the compressor were tried in the system. First, a high temperature version (Model MB-158 HT) with 186 W motor was installed in the system. However, a significant temperature rise of the process gas after compression was not achieved, probably due to high termal losses. Another version (Model MB-158) of the same blower which has similar compression characteristics and comes with a 75 W motor was substituted for the first one. Major problem with these blowers is their sensitivity to condensing vapor. The bellows tend to rupture when even a small amount of liquid condenses in them; however, this problem was partially eliminated by operating the compressor upside down. The other problem which could not be solved was the inefficiency of the motors. The motors

achieve only 30% efficiency; thus, the power requirement of even the smaller model was rather high.

Liquid Pumps

Initially a smaller gear pump which was capable of pumping about 600 ml/min urine through the system with 13 watts power requirement was installed in the system. During a later part of the testing, when the effects of urine circulation rate on the vapor production rate was investigated, this pump was replaced by a much stronger magnetic drive gear pump which can pump up to 322 L/h. For the required urine circulation rate of 950 ml/min, the existing pump is much too strong than actually needed and can be replaced with a smaller one, reducing power requirements.

System Packaging

A suitable arrangement of components minimizing the total volume of the system and shortening the connecting lines was established, and the units were mounted on a laboratory frame (56 cm x 46 cm x 94 cm). The overall view of the process package, without the insulation, is shown in Figure 33. The total weight of the system is 68 kg (150 lb). The weight of the individual components is shown in Table 17.

The components were connected with stainless steel tubing; in most cases stainless steel Swagelok fittings were used. Each component can be removed from the system for repair or service. Several manual and solenoid valves were installed for flow adjustment or diversion. Special provisions were made for by-passing some of the units (such as the evaporator) during the start-up or shut-down. The compressor and the liquid pumps were initially located in the lower section of the process package and were anchored to the base board. During the testing it was noticed that some condensation could occur in the lines leading to the compressor which might damage the bellows in the compressor. Therefore, the compressor was raised and placed upside down to eliminate the possibliity of any liquid accumulation.

The individual components and the connecting lines were heavily insulated with high temperature type refractory fiber insulating materials, then the spaces between the components were filled with the same insulating material.

The temperature controllers and a recorder were installed in an equipment rack adjacent to the process package.

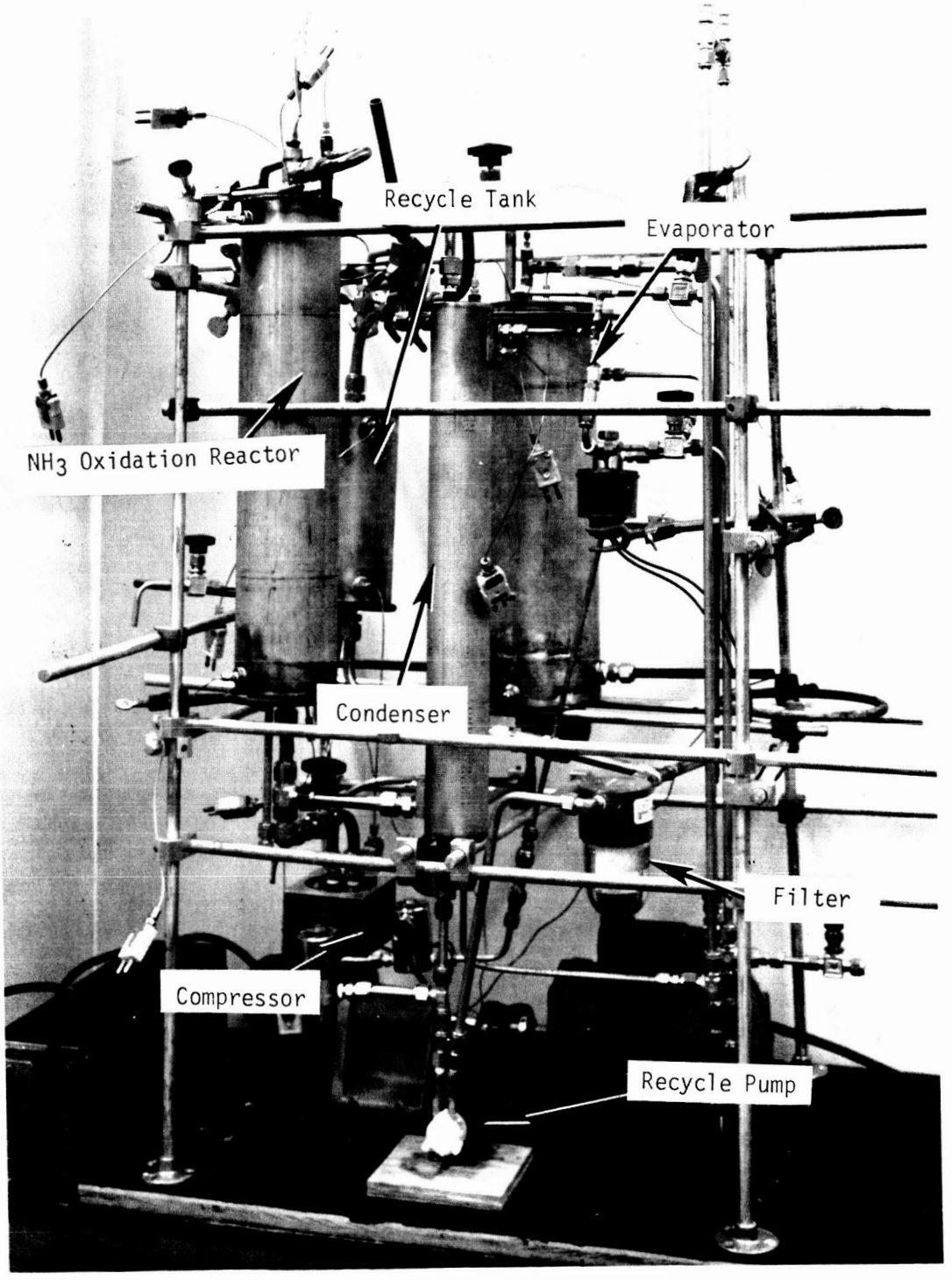

Figure 33 OVERALL VIEW OF THE PROCESS PACKAGE

TABLE 17

WEIGHT OF SUBSYSTEM COMPONENTS

Component	Weight, kg	(lb)
Evaporator	8.2	(18)
Ammonia Oxidation Reactor	5.4	(12)
Condenser	3.6	(8)
Recycle Tank	2.0	(4.5)
Compressor	6.3	(14)
Recycle Pump	2.5	(5.5)
Feed Pump	0.9	(2)
Nitrous Oxide Decomposition Reactor	0.2	(0.5)
Solenoid Valves	1.1	(2.5)
Pressure Gauges	0.9	(2)
Check Valves	0.4	(1)
Valves	0.9	(2)
Connecting Lines	3.6	(8)
Insulation	16.3	(36)
Frame	15.4	(34)
Total	67.7	(150)

Design Verification Tests

After the fabrication of the individual components, tests were performed to establish the functionality of the basic components and to ascertian their capability to operate at the design capacity levels. The results of these tests are summarized in Table 18 and indicate that the NH_3 oxidation reactor and the water condenser are capable of operating at capacities significantly above those of the design levels. However, the evaporator was operating severely below its design capacity.

TABLE 18

COMPONENT CAPACITIES

Component	Function	Capacity	
		Design	Test
NH_3 Oxid. Reactor	Flow rate, L/min	22.5	45
Water Condenser	Rate of water recovery, kg/hr	0.5	0.75
Evaporator	Urine evaporation rate, kg/hr	0.5	0.1-0.15
N_2O Decomp. Reactor	Flow rate		Adequate

Initially, Nafion (a perfluorinated ion exchange polymer) hollow fibers were selected for the evaporator. Prior to the design of the evaporator, a sample of Nafion hollow fibers (0.61 cm (0.024") ID, 0.086 cm (0.034") OD) was obtained from the original developer, DuPont Corp., for testing. A six fiber bundle (25.4 cm (10") long) was prepared and installed in a glass cylinder, then tested passing heated water through the hollow fibers and air through the glass cylinder, i.e., effectively simulating the anticipated conditions of the evaporator. The evaporation rate was established from the amount of water collected in a given time. The evaporator was then designed based on these observed evaporation rates.

A new batch of Nafion of the same size as used in the previous tests was obtained from the Permapure Products, which, meanwhile, purchased the Nafion production and distribution rights from DuPont. The initial testing of the evaporator constructed using these fibers indicated a very low evaporation rate, as compared with the previously tested Nafion fibers. Discussions with the manufacturer indicated that the fiber is manufactured in either salt or acid form and that the acid form is more permeable to water vapor. The salt form, however, can be converted to the acid form by treating with hydrochloric acid, followed by a rinse in boiling water.

One of the fiber bundles was removed from the evaporator and tested as is and after conversion to the acid form in an experimental arrangement similar to the one used previously with the initial six-fiber bundle. In addition, the original six-fiber bundle was retested, providing the same results as before.

The results of these tests are summarized in Table 19. The evaporation rate of the full-size bundle was lower than that of the six-fiber bundle by an order of magnitude. Even the acidified fibers showed much lower rates than the original six-fiber bundle. After all this testing, the only explanation is that the hollow fibers are non-uniform and vary from batch to batch; apparently the transfer of the fiber production to another company resulted in hollow fibers with very much different properties.

In addition to these Nafion fibers, other materials were investigated. Hollow fibers made from Teflon showed extremely low evaporation rate. Polysulfone fibers showed very high production rate; however, most of the water was transferred in a liquid form. In addition, polysulfone fibers have a high sodium chloride permeability. Dow Chemical Co. and Monsanto are actively working in the development of hollow fibers with high water vapor permeabilities; however, they anticipate to have samples only by the end of 1985.

In view of the above described results, and with the concurrence of the technical project monitor, it was decided to use the available Nafion hollow fiber bundles, knowing that the production rate will be below the anticipated value.

TABLE 19

VAPOR PERMEATION THROUGH HOLLOW FIBERS

Type of Bundle	Pressure, MPa (psia)	Water		Air Flow Rate, cm^3/min	Water Recovery Rate, g/hr
		Flow Rate, ml/min	Inlet Temp., °K (°F)		
Six-Fiber Bundle (25.4 cm long)	0.0267 (3.86)	35	344 (160)	-	10.8
	0.0307 (4.45)	30	350 (171)	-	9.0
	0.0787 (11.41)	30	350 (171)	50	13.1
	0.0800 (11.60)	35	352 (174)	50	13.8
	0.0800 (11.60)	30	333 (140)	50	9.0
	0.0680 (9.86)	30	336 (145)	50	3.5
	0.0680 (9.86)	30	338 (149)	50	3.7
120-Fiber Bundle (25.4 cm long) (water inside the fiber)	0.0680 (9.86)	110	338 (149)	570	21.4
	0.0680 (9.86)	300	338 (149)	570	25.6
	0.0680 (9.86)	500	338 (149)	570	25.7
	0.0680* (9.86)	500	338 (149)	570	29
	0.0680* (9.86)	500	347 (165)	570	29
	0.0680* (9.86)	110	347 (165)	570	43.7
120-Fiber Bundle (water outside the fiber)	0.0680* (9.86)	500	338 (149)	570	29
	0.0680* (9.86)	500	347 (165)	570	50

* After treatment with the HCl and boiling water

SUBSYSTEM TESTING

The testing program consisted of the following test series.

1. Parametric testing to determine the effect of various operational parameters on the overall performance of the system and to establish the optimum operational conditions,

2. Daily endurance tests for one month,

3. Continuous operation for 7 days (168 hr).

All tests were performed using feed of untreated urine collected daily from male volunteers. Sampling and analysis were performed to obtain the processing rate and to determine the quality of the recovered water. Typically, the following analyses were performed:

a) Recovered water - the quality of water was monitored by routinely testing for pH, NH_3, organic carbon (TOC), conductivity, nitrite and nitrate.

b) Vent gas - selected samples were analyzed for N_2O.

c) Feed - selected batches were analyzed for specific gravity, total solids, urea, ammonia and inorganic solids. For the continuous run, proportionate samples of feed were frozen and the tests were performed on the composite sample,

d) Sludge - analyzed for specific gravity, total solids, volatile solids, inorganic solids, urea, and ammonia.

The following analytical techniques were used.

a) A gas chromatographic method using Electron Capture Detector and a Porpak Q column was used for measuring the N_2O concentrations.

b) The organic carbon was determined by Beckman total organic carbon analyzer.

c) Ammonia in the recovered water was determined by Nesslerization method using Chemtrics, Inc. vacu-vials. After the development of color, ammonium ion concentration in the water was measured from spectral absorbance at 530 nm using Bosh & Lamb Spectronic 20 analyzer.

d) Nitrite and Nitrate in the recovered water was determined by kit obtained from Chemtrics, Inc.

In addition, combined samples of the recovered water were submitted to a commercial laboratory for an independent check on TOC.

Parametric Testing

Two types of parametric tests were performed:

1. Water quality - The independent variables for water quality are NH_3 oxidation reactor temperature, oxygen concentration and evaporator pressure (which determines the mass flow or space velocity),

2. Water production rate - The independent variables are evaporation temperature, evaporator pressure and urine recirculation rate.

To minimize the number of tests, an experimental plan based on a two-level factorial design with so-called star points at distances from the center equal twice to normal variable level steps was chosen. This technique is described in standard texts on experimental design and was successfully used on other programs. This approach allows to determine the effects of independent variables in a statistically acceptable manner and satisfies the requirements for the development of a quadratic polynomial for expressing the values of the chosen dependent variable. To eliminate the effect of solids content, each test was performed using fresh urine.

Parametric Testing for Water Quality.- The quality of the recovered water obtained during these tests is shown in Table 20. The effects of each variable are as follows:

Temperature - The minimum temperature required for the removal of ammonia was 527°K (489°F). However, when one of the runs was repeated, higher level of ammonia was observed in the recovered water. Therefore, the catalyst temperature was raised to 544°K (520°F) and all further testing was performed at that temperature.

Oxygen Concentration - To protect the oxygen analyzer's sensor against the high temperature in the recycle line, the sensor is installed in the vent stream. The oxygen concentration in the recycle stream is calculated from the measured oxygen concentration in the vent gas and the water condensation rate. Due to the low oxygen consumption of the system, the oxygen concentration circulating in the system even at low oxygen feed flow rates is high. Therefore, during some tests nitrogen was supplied to the system to adjust the oxygen concentration to desirable levels and to determine the minimum required oxygen concentration for the removal of ammonia. Because of the operational difficulties, the oxygen concentration could be lowered only to about 5%, and no change in the water quality was observed.

TABLE 20

PARAMETRIC TESTS FOR WATER QUALITY

Test No.	Ammonia Catalyst Temp., °K (°F)	Oxygen in the Recycle Stream, %	Evaporator Pressure, kPa	Recovered Water Analysis				
				pH	Ammonia, mg/L	T.O.C. mg/L	Specific Conductance, μ mho/cm	Nitrite & Nitrate, mg/L
Catalyst Temperature								
13	566 (559)	14	93.1	4.57	0.08	<2.0	21	>5.0
14	544 (520)	14	93.1	4.68	0.08	<2.0	24	3.4
17	527 (489)	14	93.1	4.67	0.09	<2.0	26	3.5
16	511 (460)	14	93.1	4.70	0.90	3.0	28	3.5
20	527 (489)	14	81.4	4.71	0.07	4.0	21	3.2
21	527 (489)	14	81.4	6.2	1.8	5.0	35	3.2
Oxygen Concentration								
27	544 (520)	15	85.5	4.52	ND	5.0	14	1.0
28	544 (520)	8	85.5	4.71	0.2	<2.0	18	2.0
29	544 (520)	5	85.5	4.60	0.02	<2.0	19	2.0
Evaporator Pressure								
14	544 (520)	14	93.1	4.68	0.08	<2.0	24	3.4
23	544 (520)	14	89.6	4.62	0.13	<2.0	19	1.5
24	544 (520)	14	89.6	4.72	0.12	<2.0	23	1.5
27	544 (520)	14	85.5	4.52	ND	5.0	14	1.0
25	544 (520)	14	81.4	4.68	0.17	2.0	23	1.5
15	527 (489)	14	93.1	4.66	0.21	3.0	23	3.5
22	527 (489)	14	89.6	4.60	0.08	3.0	22	3.2
19	527 (489)	14	85.5	4.68	0.07	2.5	24	3.0
20	527 (489)	14	81.4	4.71	0.07	4.0	21	3.2

ND = Not Detectable

Evaporator Pressure - The evaporator pressure determines the mass flow rate through the ammonia oxidation reactor. The evaporator pressure was varied between 81.4 and 93.1 kPa. The quality of the water remained the same through this range.

Parametric Testing for Water Production Rate. - The results of these tests are presented in Table 21. Based on these results, the following linear expression relating the production rate to the independent variables was developed:

$$Y = -429.1 + 2.25T + 0.0085F - 2.719P \qquad (10)$$

where Y = production rate in ml/hr, T = evaporation temperature in °K, F = urine circulation rate in ml/min, and P = evaporation pressure in kPa. The quality of water produced was good under all the conditions of parametric testing.

The evaporation temperature has the most significant influence on the production rate; however, the need for mechanical stability of the evaporator fibers restricts the upper temperature limit at 344°K (160°F), which is considered relatively safe for the fibers. Although the production rate is increased by a decrease in the evaporator pressure, the capability of the compressor determines the lowest pressure practically achievable (approximately 93 kPa). Among the independent variables, the urine circulation rate has the least influence on the production rate. The conveniently achievable variation rate of 950 ml/min was chosen for further testing.

Daily Endurance Tests

The daily endurance testing was continued for one month, with system startup, operation and shutdown based on an 8-hour workday basis. Initially, the urine recycle loop of the system was filled with fresh, untreated urine, then fresh urine was added continuously during the tests to maintain its volume recycling within the system; therefore, the solids content within the recycle loop increased continuously. The system was restarted every morning, water collection continued for 5-6 hours, and shut down for the night. Normally, the presence of an operator was required for startup and shutdown; at other times the system operated essentially unattended. Sampling and analyses were performed to determine the processing rate, the quality of the recovered water, and to obtain material balance.

TABLE 21

PARAMETRIC TESTS FOR WATER PRODUCTION RATE

Run No.	Evaporation Temperature, °K (°F)	Urine Circulation Rate, ml/min	Evaporator Pressure, kPa	Recovered Water, ml/hr
39	341 (154)	800	96	85
43	347 (165)	1100	96	100
40	347 (165)	800	93	105
34	341 (154)	1100	93	95
42	344 (160)	950	93	105
45	344 (160)	950	93	108
44	344 (160)	950	94	90
36	347 (165)	800	93	110
41	344 (160)	950	93	110

Table 22 summarizes the results of the daily endurance testing. The overall water recovery efficiency of the system is 96.1% and the vent loss is 0.5%. The material balance for the entire test is summarized in Table 23. Since urine was collected only during the daytime, the solids concentration of feed was found to be somewhat lower than usually assumed for a normal urine. The total solids concentration in the recycle stream sludge increased to 110.8 g/L (or 10.48% on the weight/weight basis). The volatile residue consists of all organic materials plus urea, i.e., materials that are volatilized during the standard analytical procedures for solids. It can be seen that there was a loss of both organics and urea, as it should be if some of the urea is decomposed and the produced ammonia and volatilized hydrocarbons are oxidized in the catalytic reactor.

The quality of the recovered water (without any posttreatment) is shown in Table 24, where the measured ranges of the daily tests are presented together with the analysis of the total combined volume of water collected during this entire test series. Selected samples of the vent gas were analyzed for the presence of N_2O (nitrous oxide). In a typical test, the N_2O concentration in the gas stream prior to N_2O decomposition reactor was in the 1000-1300 ppm range; however, the actual vent (i.e., after passing the N_2 decomposition reactor) contained only 50-200 ppb (parts per billion) of N_2O. This concentration is below the N_2O concentration in normal air (approximately 250 ppb) and below that in the feed oxygen gas used (approximately 300 ppb).

Continuous Operation

The continuous operation test was run for 168 consecutive hours. At the beginning, the urine recycle loop of the system was filled with fresh, untreated urine, then untreated urine was added continuously during the test to maintain its volume within the recycle loop. After startup, the system operated completely automatically; it was attended only during the normal day working hours and was left to operate unattended during the nights and weekend. Except for a temporary rise in temperature of the recycling urine to levels higher than normal on the morning of the second day of operation (probably due to an undetermined malfunction of the temperature controller during the night), the system operated very smoothly and required no adjustments during the entire test period.

The quantity of the recovered water was measured daily, and its quality was routinely checked by daily analyses. The experimental water recovery data of the continuous test are summarized in Table 25. The observed efficiency of water recovery is 94.7%, which is somewhat lower than the efficiency achieved during the daily test series. It is suspected that some vapor may have escaped through the overpressure

TABLE 22

EXPERIMENTAL DATA OF THE ENDURANCE TESTING

Test No.	Test Duration, hr	Urine Feed, ml	Recovered Water, ml	Vent Loss, ml
46	5	480	515	1.5
47	6	685	665	1.5
48	4	580	510	0.5
49	4	470	500	12
50	5.83	500	280	0.5
51	5.50	970	504	0
52	6.75	0	343	3
53	6.08	550	603	0
54	5	500	475	3
55	6	570	545	2.5
56	6	560	510	3.5
57	6	550	510	8
58	6	550	535	1.5
59	6	570	540	1.5
60	6	550	510	1.5
61	6	550	510	2
62	6	550	505	1
63	6	540	530	2
64	6	520	505	2
65	6	510	485	9
Total	114.17	10755	10080	56.5

Recoverable water Feed, g	10485		
Collected water, g			10080
Recovery efficiency, %		96.1	
Vent loss, %			0.5

TABLE 23

MATERIAL BALANCE FOR FEED AND SLUDGE OF THE ENDURANCE TESTING

Parameter	Feed	Recovered in Sludge
Specific gravity, g/cm^3		1.0569
Solid content, g/L	26.5	110.8
Total solids, g	362	319
Inorganic solids, g	139	150
Volatile residue (organic + urea), g	223	169
Urea, g	131	110

TABLE 24

ANALYSIS OF THE WATER RECOVERED
DURING THE ENDURANCE TEST

Parameter	Range of Daily Collections	Combined Pool
Ammonia, mg/L	0.02-1.2	0.09
Total Organic Carbon, mg/L	< 2	< 2
pH		5.35
Specific Conductance, μmho/cm	16-27	18
Nitrite and Nitrate, mg/L	2.0-3.5	3

TABLE 25

EXPERIMENTAL DATA OF THE CONTINUOUS TEST

Date	Time	Feed Added Between the Time Intervals, ml	Water Collected		Vent Loss, ml
			Total, ml	Average Rate, ml	
8/19/85	12:30 pm	400	start		
8/20/85	12:30	4300	2170	90.4	13
8/21/85	12:30	2200	2285	95.2	8
8/22/85	12:30	2100	2255	93.9	7
8/23/85	12:30	2300	2050	85.4	7
8/24/85	12:30	2400	2060	85.8	7
8/25/85	12:30	2100	2035	84.8	8
8/26/85	12:30	290	1970	82.1	9
Volume Correction		-172			
Total		15918	14825	88.2	59
Recoverable water in the Feed, g		15655			
Recovered Water, g			14825		
Efficiency, %		94.7			
Vent Loss, %					0.38

protection valve of the liquid recycle loop during the period of abnormal temperature of the urine (363°K (194°F) instead of 344°K (160°F)) mentioned above. Such an increase in temperature may have caused a sufficient increase in pressure to open the valve, resulting in loss of vapor.

The quality of the recovered water is presented in Table 26; there was no change in the quality of water during the entire test, i.e., no dependence on solids content of the recirculating urine. Random samples of the vent gas and of oxygen feed were analyzed for N_2O. The results are summarized in Table 27 and indicate that the N_2O concentrations in vent are, generally, equal or lower than its concentrations in feed oxygen and are in the range of N_2O levels of ambient air.

The material balance of solids is summarized in Table 28. As anticipated, there is a loss of total solids in the form of volatile organics, urea, and ammonia. Obviously these materials evaporated together with the water and were converted to innocuous products in the catalytic reactors.

Analysis of Experimental Results

Water Quality.- The analysis of water collected during the daily endurance and the continuous 168 hours long tests is summarized in Table 29, together with current EPA drinking water primary and secondary standards and NASA specifications for space station water (obtained from Mr. Ch. Willis, Technology Incorporated). Daily water analysis indicated that the increase in solids content of the recirculating urine has no influence on the quality of the recovered water. As Table 29 indicates, the recovered water is of good quality and, with the exception of a low pH, meets EPA potable water standards and approach the NASA proposed revised standards without posttreatment. The pH can be easily adjusted either by addition of alkalies or by passing water through ion exchanger or limestone chip column. The expendables required for the adjustment of pH to a neutral value are approximated at 1 g per liter of water.

Since the recycling urine is maintained above the pasteurization temperature (i.e., above 338°K (149°F)) and the vapor passes through the catalyst bed at 523°K (482°F), the recovered water does not show any viable bacteria.

Material Balance.- A typical material balance required for producing one (1) kilogram of water is shown in Figure 34. Average data of the daily and the continuous runs were used for this analysis. During these tests, the observed average water collection efficiency was 95.4%, and 0.5% of water was lost with the vent gases. Approximately 15% of the urea

TABLE 26

ANALYSES OF THE WATER RECOVERED
DURING THE CONTINUOUS TEST

Parameter	Range of Daily Collections	Combined Pool
Ammonia, mg/L	0–0.12	0.08
Total Organic Carbon, mg/L	<2	< 2
pH		5.49
Specific Conductance, μmho/cm	16–24	17
Nitrite and Nitrate, mg/L	1.5	1.5

TABLE 27

N_2O CONCENTRATION IN VENT GAS

Sample Date	Vent N_2O, ppb	Oxygen Feed N_2O, ppb
8/22/85	373	774
8/23/85	229	258
	287	287
8/26/85	<50	216
	<50	192

TABLE 28

SOLIDS MATERIAL BALANCE FOR
CONTINUOUS TEST

Parameter	Feed	Recovered in Sludge
Specific gravity, g/cm^3	1.015	1.0813
Solid content, g/L	31.5	179.4
Total solids, g	590	517
Inorganic solids, g	215	213
Volatile residue (organic + urea), g	375	304
Urea, g	246	225
Ammonia, g	20	14

TABLE 29

SUMMARY OF WATER QUALITY

Parameter	Pool Continuous Test	Pool Daily Runs	EPA Primary & Secondary Standards	NASA Proposed Revised Stand.
Ammonia, mg/L	0.08	0.09	-	< 0.5
Total Organic Carbon, mg/L	<2	<2	-	0.1
pH	5.5	5.3	10	10
Specific Conductance, μmhos/cm	17	18		3.3
Nitrate & Nitrite, mg/L	1.5	3	6-8	6-8

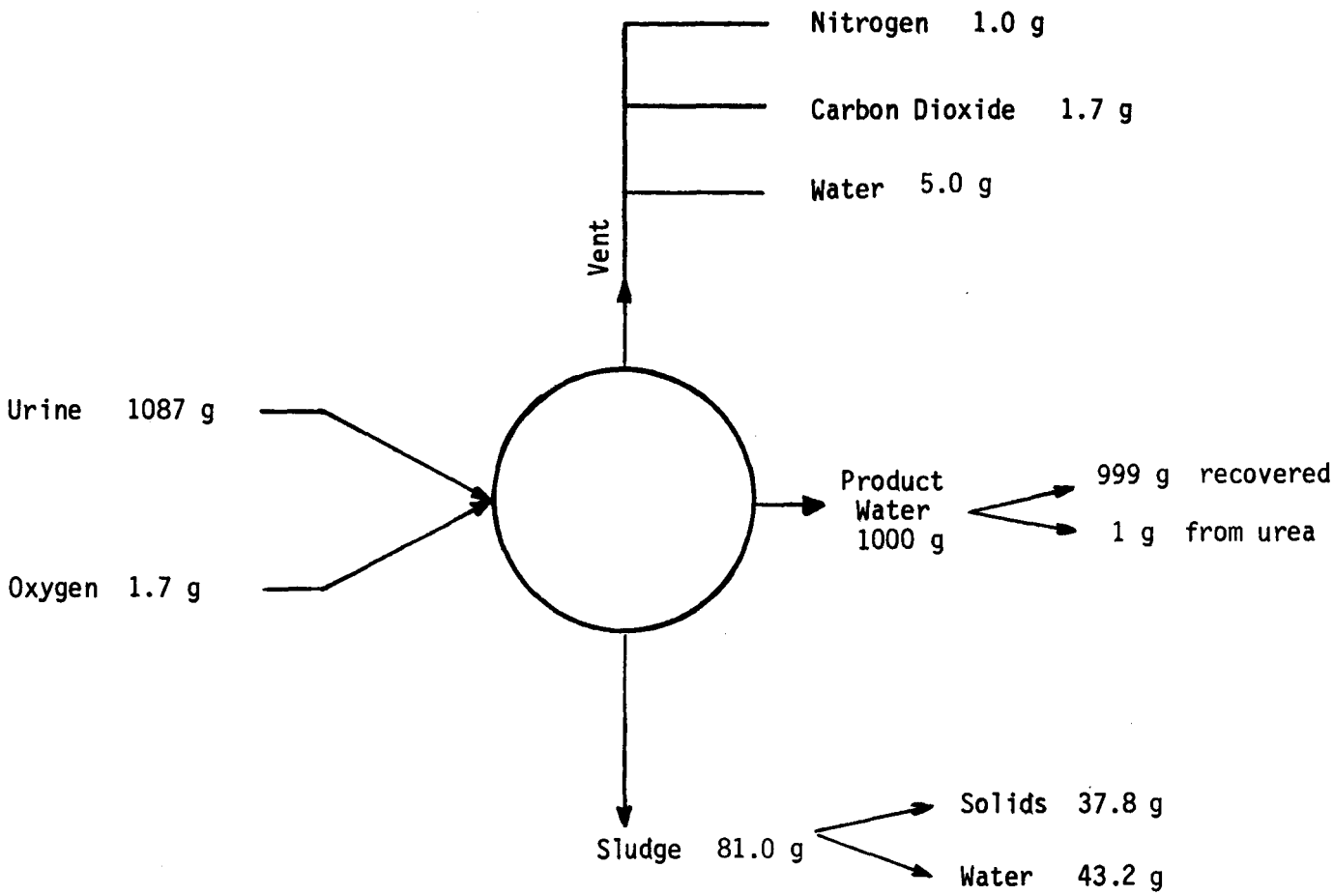

Feed:
1088.7 g

Products:
1088.7 g

Figure 34 PROCESS MASS BALANCE

decomposed and produced ammonia which was oxidized to nitrogen and water. The destruction of urea proceeds according to the following overall equation:

$$H_2NCONH_2 + 1.5\ O_2 \longrightarrow N_2 + CO_2 + 2\ H_2O$$

with appropriate values reflected in Figure 34. The amounts of total sludge and sludge solids are derived from values obtained during these tests. Because no pretreatment of urine is required, the only expendable for the process is oxygen.

Production Rate.- Because of severely undersized evaporator (for reasons explained in previous chapters), the water production rate was only approximately 100 g/hr; this rate indicates an evaporation rate of approximately 14 g/hr per square meter of surface area of the hollow fibers. Because the evaporator temperature was maintained constant, the evaporation (and, consequently, the production rate) decreased with the increase in the solids content of the recycling urine, as shown in Figure 35.

Individual testing of other components which could affect the production rate (water condenser, blower/compressor, catalytic reactor) indicated that these components meet and/or exceed the design values; therefore, a redesigned evaporator with an adequate evaporating surface would allow to operate the system at the design 3-man rate.

Energy Requirements.- The design and observed power requirements for various components and for the entire system are presented in Table 30. Due to low vapor production rate of the evaporator, meaningful energy requirements (W-hr/kg) could not be obtained; therefore, power units (i.e., watts) were used in Table 30. The system operates in such a manner that increasing the water production rate to the design value by adding more evaporation fibers would not increase the power requirements of individual components; thus, would result in a decrease of energy requirements for the water produced.

The large differences between the design and actual data are caused mainly by the inefficiency of the bellows compressor/blower. First, the motor of the compressor/blower operates at approximately 30% efficiency (115 V, 2.1 A, 75W). Second, due to the configuration and bulkiness, there are excessive heat losses both from the air cooled motor and from the blower head; thus, the expected preheating of the recycle gas/vapor stream due to compression could not be achieved and the preheating of the gas/vapor entering the NH_3 oxidation reactor had to be done by an electric heater. Since the theoretical compression energy required is approximately 66 W-hr/kg. of vapor, an application of high efficiency

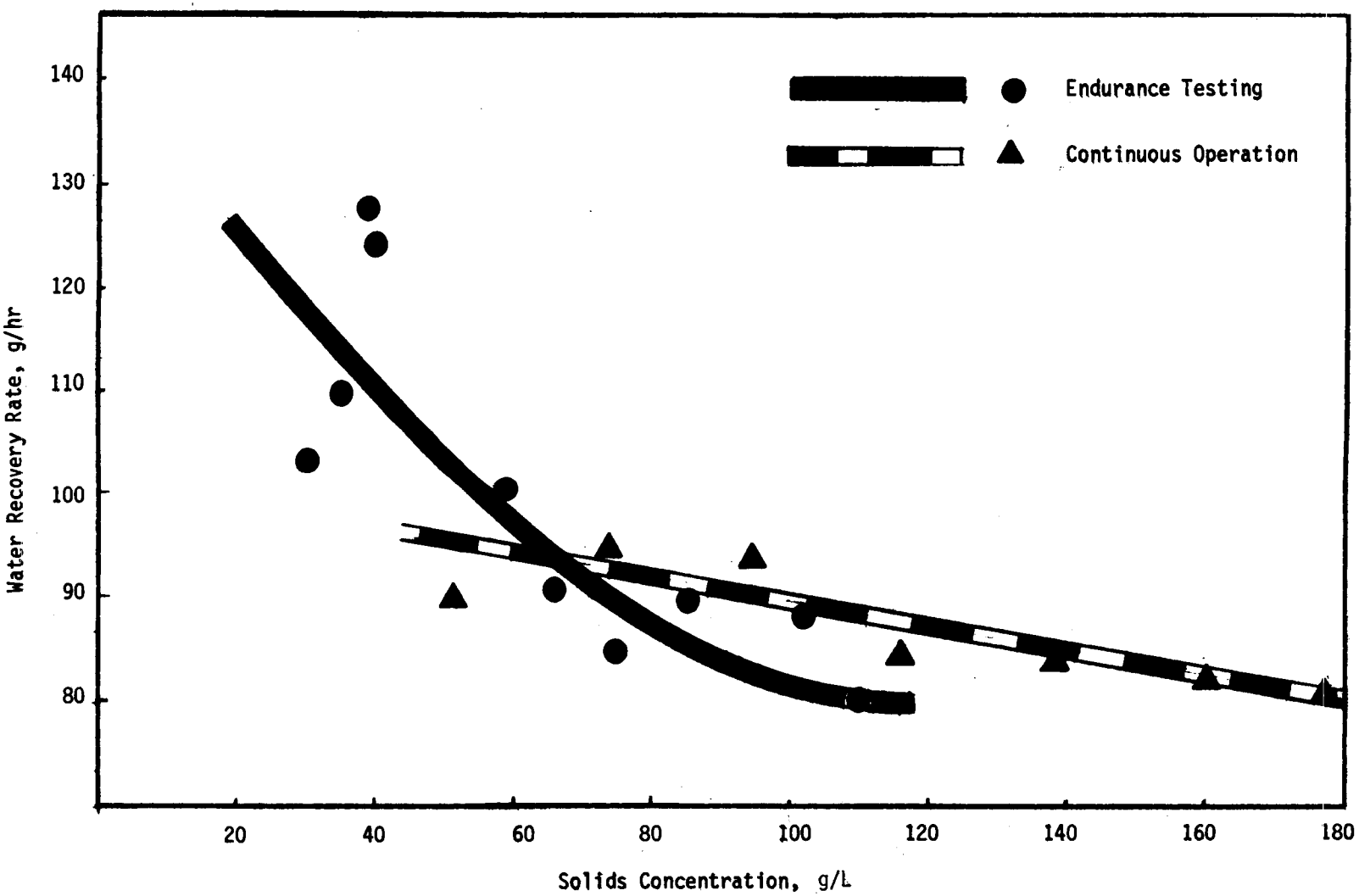

Figure 35 EFFECTS OF SOLIDS CONCENTRATION ON WATER PRODUCTION RATE

TABLE 30

POWER REQUIREMENTS

Component	Actual Power, W	Design Power, W
a) Subsystem Power		
Liquid Pumps	13-42	30
Compressor	152	82
Liquid Heater	6	0
NH_3 Reactor Heater	47	7
N_2O Reactor Heater	20	0.4
Total	267	119.4
b) Instrumentation & Controls	27	27

motor would bring the energy requirements of the compressor/ blower to the design value.

The second reason for high energy requirements are due to the combined effect of thermal wall losses and low production rate. Since the system components are maintained at specific temperatures, the thermal wall losses are constant regardless of the production rate. An increase in the production rate would decrease the specific energy requirements.

The third problem was that the heat exchanger of the N_2O decomposition reactor did not function because of a very low vent rate, and all the heat had to be supplied by an electric heater. Here, again, a very small percentage of the heat was required to preheat the vent gases to the reactor temperature and essentially all the energy was expended for maintaining the temperature of the reactor, i.e., mainly heat loss to ambient. A reconfiguration of this reactor to allow its heat losses to be used for preheating the vapor entering the NH_3 oxidation reactor would significantly reduce the overall energy requirements.

Correcting the above listed deficiencies, i.e., obtaining an efficient blower/compressor, increasing the evaporator size, and relocation of the N_2O decomposition reactor, would allow to meet the design energy requirements.

Comparison With Other Systems

A comparison of the vapor phase ammonia removal system (VPCAR) with other water recovery system (VCD, TIMES) is difficult because:

a. This is the first generation engineering breadboard system fabricated entirely from commercially available components, while the VCD and TIMES are 3rd or 4th generation system and have already reached the pre-prototype stage,

b. Literature on VCD and TIMES usually describe the systems only, without taking into account the penalties associated with hardware and expendables required for urine pretreatment and posttreatment, which are not required for the VPCAR system.

Tables 31 and 32 compare the three water recovery systems and the quality of the water produced by each system. Data for VCD and TIMES were taken from an analysis by F.H. Schubert, "Phase Change Water Recovery Techniques: Vapor Compression Distillation and Thermoelectric/ Membrane Concepts" presented at the Thirteenth Intersociety Conference on Environmental Systems, San Francisco, Ca., July 11-13, 1983. Data for this system (VPCAR) are for an unoptimized engineering breadboard system.

TABLE 31

COMPARISON OF WATER QUALITY

Parameter	This System (VPCAR)	VCD	TIMES
Ammonia, g/L	0.09	0.3	0.8
Total Organic Carbon, g/L	< 2	16-80	48-150
pH	4.5-5.5	3-4	3.3-3.6
Conductivity, μmhos/cm	18	35	198

TABLE 32

COMPARISON OF WATER RECOVERY SYSTEMS

Parameter	This System (VPCAR)	VCD	TIMES
System weight, kg (lb)	68 (150*)	93 (205)	68 (150)
System volume, m^3 (ft^3)	0.24 (8.5*)	0.44 (15.7)	0.23 (8.0)
Specific energy, W-hr/kg (W-hr/lb)	217 (98.5**)	101 (46)	203 (92)
Water recovery, %	95.4	95.5	91.4
Vent/purge losses, %	0.5	0.5	3.0
Expendables			
Urine pretreatment, g/L	0	7.3	7.3
Oxygen, g/L	5.7	0	0
Urine filter, g/L		same	
Solids buildup in sludge, g/L	32	44	44
Posttreatment			
pH adjustment, g/L		same	
TOC removal	no	yes	yes
Inorg. removal	no	yes?	yes?
Control instrumentation		same	

* Commercially available components
** Design Value

Wherever quantitative data were unavailable, qualitative statements were used for each system.

As can be seen from Tables 31 and 32, the engineering breadboard of this system (VPCAR) produces water of superior quality, has lower requirements for expendables, and has lower accumulation of sludge; at the same time, it is competitive with other systems in weight, volume, and power requirements. Additional development of this system to pre-prototype stage would further improve its competitive position.

CONCLUSIONS

Data developed during the design, fabrication, and testing of an integrated engineering breadboard subsystem for the recovery of potable water from untreated urine leads to the following conclusions.

1. The overall operation of the integrated system has been demonstrated. As shown by the 168-hour long test of continuous operation, the subsystem is capable of automatic operation for prolonged period of time.

2. The process based on catalytic distillation for vapor phase catalytic ammonia removal produces water of good quality from untreated urine. The recovered water has a quality superior to water produced by other systems, such as VCD or TIMES, and requires only a pH adjustment for meeting the USEPA primary and secondary potable water standards.

3. Because of an underdesigned evaporator, the desired production rate could not be demonstrated. Since the capacities of other subsystem components were at or above the design 3-man rates, an adequate increase in the surface area of the evaporator hollow fibers would allow to reach the 3-man production rate.

4. Because of a combined effect of low production rate and inefficiency of the commercially available blower/compressor used, meaningful determination of the specific energy requirements could not be made.

5. The water recovery subsystem employing catalytic distillation for vapor phase catalytic ammonia removal is competitive with VCD and TIMES systems. This process produces good water, does not require pretreatment of urine, and needs less expendables than other methods. Although the subsystem was not optimized, its weight and volume are in the same range as those of VCD and TIMES; the specific power-requirements could be brought to the same range after further development of blower/compressor and installation of a larger evaporator.

6. Based on the above, further development of the vapor phase catalytic ammonia process to a pre-prototype status is warranted.

1. Report No.	2. Government Accession No.	3. Recipient's Catalog No.
NASA CR-177382		

4. Title and Subtitle	5. Report Date
CATALYTIC DISTILLATION WATER RECOVERY SUBSYSTEM	September, 1985
	6. Performing Organization Code

7. Author(s)	8. Performing Organization Report No.
Pranas Budininkas and Firooz Rasouli	
	10. Work Unit No. T-6937
9. Performing Organization Name and Address GARD Division, Chamberlain Manufacturing Corp. 7449 N. Natchez Avenue Niles, Illinois 60648	11. Contract or Grant No. NAS2-11687
	13. Type of Report and Period Covered Contractor Report
12. Sponsoring Agency Name and Address National Aeronautics and Space Administration Washington, DC 20546	14. Sponsoring Agency Code 506-64-31

15. Supplementary Notes

Point of Contact: Technical Monitor, Ted Wydeven, MS239-4
Ames Research Center, Moffett Field, CA 94035
(415) 694-5738 or FTS 464-5738

16. Abstract

An integrated engineering breadboard subsystem for the recovery of potable water from untreated urine based on the vapor phase catalytic ammonia removal was designed, fabricated and tested. Unlike other evaporative methods, this process catalytically oxidizes ammonia and volatile hydrocarbons vaporizing with water to innocuous products; therefore, no pretreatment of urine is required. Since the subsystem was fabricated from commercially available components, its volume, weight and power requirements were not optimized; however, it is suitable for zero-g operation. The testing program consisted of parametric tests, one month of daily tests and a continuous test of 168 hours duration. The recovered water is clear, odorless, low in ammonia and organic carbon, and requires only an adjustment of its pH to meet potable water standards. The obtained data indicate that the vapor phase catalytic ammonia removal process, if further developed, would also be competitive with other water recovery systems in weight, volume and power requirements.

17. Key Words (Suggested by Author(s))	18. Distribution Statement
Water Recovery from Urine, System for Water Recovery, Catalytic Distillation, Catalytic Ammonia Removal	Unclassified - Unlimited Subject Category 54

19. Security Classif. (of this report)	20. Security Classif. (of this page)	21. No. of Pages	22. Price*
Unclassified	Unclassified	97	

*For sale by the National Technical Information Service, Springfield, Virginia 22161